CZECH TECHNICAL UNIVERSITY IN PRAGUE

FACULTY OF MECHANICAL ENGINEERING

DOCTORAL THESIS STATEMENT

CZECH TECHNICAL UNIVERSITY IN PRAGUE

FACULTY OF MECHANICAL ENGINEERING

DEPARTMENT OF AUTOMOTIVE, COMBUSTION ENGINE AND RAILWAY ENGINEERING

DISSERTATION THESIS STATEMENT

Phenomenological Combustion Modeling for Optimization of Large 2-stroke Marine Engines under both Diesel and Dual Fuel Operating Conditions

Ing. Filip Černík

Doctoral Study Program: Mechanical Engineering

Field of Study: Machines and Equipment for Transportation

Supervisor: prof. Ing. Jan Macek, DrSc.

Dissertation thesis for the academic degree of ”Doctor“, abbreviated to "Ph.D."

Prague February 2018

The present dissertation thesis was elaborated in the combined form of doctoral studies at the Department of Automotive, Combustion Engine and Railway Engineering, Faculty of Mechanical engineering, CTU in Prague.

Candidate: Ing. Filip Černík

Department of Automotive, Combustion Engine and Railway Engineering, Faculty of Mechanical Engineering, CTU in Prague

Technická 4, CZ 166 07 Praha 6, Czech Republic

Supervisor: prof. Ing. Jan Macek, DrSc.

Department of Automotive, Combustion Engine and Railway Engineering, Faculty of Mechanical Engineering, CTU in Prague

Technická 4, CZ 166 07 Praha 6, Czech Republic

Thesis copies were distributed on: .....

Dissertation Thesis Defense takes place on ..... at ……...

in the Conference Room No. 17 (ground floor), Faculty of Mechanical Engineering, CTU in Prague, Technická 4, Praha 6

in front of the Dissertation Defense Committee in the Field of study: Machines and Equipment for Transportation

Dissertation thesis is available at the Department of Science and Research of the Faculty of Mechanical Engineering, CTU in Prague, Technická 4, Praha 6

doc. Ing. Oldřich Vítek, Ph.D.

Chairman of Branch Board

Machines and Equipment for Transportation

Faculty of Mechanical Engineering, CTU in Prague

1. Introduction

Stringent environmental regulations, extensive customer requirements and high market volatility force engine manufacturers to strive for new and innovative ways of improving engine performance and reducing emissions at the same time. Diesel direct injection compression ignition (DICI) engines are considered a well proven means of converting primary energy, which are in productive use in numerous applications and have been continuously further developed and optimized over the past decades. In view of the overall trend towards decarbonization, the role of diesel engines is being gradually challenged, especially in road transport. However, for marine applications, large 2-stroke low speed diesel engines remain essential, as shipping is the by far most effective means of transportation in terms of CO_2 emissions per unit load. Nonetheless, there is an undisputed need for further development in this sector as well, specifically for reducing emissions, which is a particular challenge in view of the low quality fuels predominantly used.

The introduction of the very stringent IMO Tier III emissions regulation within the revised MARPOL Annex VI [1] triggered an immense number of activities at marine engine manufactures in order to develop concepts and strategies in compliance with these new environmental standards. For large marine 2-stroke engines, where heavy fuel oil (HFO) has been the primary energy source for decades, this required the adoption of either exhaust gas aftertreatment systems or advanced exhaust gas recirculation technologies. Both options are associated with a non-negligible increase of investment as well as operational cost and the applicability in combination with HFO must be considered at least questionable. Hence, the use of alternative gaseous fuels suddenly became a viable option in that it enables to meet IMO Tier III emission limits without any need of exhaust gas aftertreatment or recirculation. In this respect, the dual fuel (DF) combustion concept combines benefits from operation on both liquid and gaseous fuels and thus represents an attractive alternative to a conventional diesel engine. Although there have been several attempts in the past to master and industrialize large marine 2-stroke DF engines, they have failed mainly because it never became economically viable to use gas instead of HFO in merchant marine applications. Obviously, the adoption of DF technology for large 2-stroke engines is also associated with some technical challenges. However, the situation has changed dramatically and recent studies have confirmed the feasibility of such a concept with all its benefits by means of numerous experimental validations on multi-cylinder test and production engines introduced to the market [2].

In view of the considerable increase of the number of technology options and corresponding design variants as well as parameter variations associated with modern, electronically controlled subsystems, the need for appropriate tools in order to reduce this number to a manageable extent is evident. Hence, more than ever before, comprehensive and predictive fast cycle simulation tools are required within engine development and optimization processes for pre-assessing both performance and emission formation associated with individual measures. Integration of such generic and fast running engine models at the early stage of development projects helps to accelerate and facilitate the development of propulsion concepts addressing the requirements dictated by the market and continuously evolving legislation.

However, such fast running and predictive computational models have not been available up to now for supporting the development of large 2-stroke marine engines. For the diesel engines, this is due to the complexity of the combustion system characterized by the presence of multiple peripheral injectors. Similarly, also the DF combustion is distinguished by a high level of complexity related to the deviation from both stoichiometric and homogenous conditions, and the combined occurrence of diffusive and premixed burning processes. In this context, extensive

experimental as well as computational investigations conducted recently are of particular benefit: They allow to gain better understanding and capture the phenomenological aspects of the various combustion concepts in large low speed 2-stroke engines and their results can be utilized for model development and validation. For instance, the outcome of comprehensive basic spray research in a dedicated spray combustion chamber [3,4] must be considered instrumental for the derivation of corresponding quasi-dimensional mathematical models in order to describe the impact of spray interactions on the diesel combustion progress. Such approach is prerequisite for a rigorous and generic combustion model definition under both diesel and dual fuel operating conditions. In this respect, it is necessary to appropriately determine the turbulent flow field characteristics, which is governing both mixing controlled diffusion combustion and turbulent premixed flame propagation. The validity of the approach finally has to be demonstrated by means of integration of the developed models in a suitable performance simulation tool and their validation against a relevant set of validation data from full engine tests.

2. State of the Art

Numerous authors have proposed physics-based and yet not time-consuming simulation concepts addressing individual phenomena of diesel combustion [5,6,8,14,15]. These range from widely used empirical approaches, often employing a Vibe function, to phenomenological models, mostly in combination with multi-zone considerations. Whereas the former are by nature not capable of satisfying requirements for physical and generic combustion predictions, phenomenological models capture physics with much higher fidelity. Multi-zonal models further extend the capability to account for detailed physics and spatial effects. However, even the most advanced of these models cannot be considered fully generic since they involve sets of model constants that need to be tuned based on experimental data or multidimensional CFD calculations. Case and engine specific model constants are used for model tuning and hence limit the model's validity and prevent its general use. Compared to detailed and computationally expensive CFD simulations, the lower model complexity of empirical and phenomenological approaches increases the demand for model tuning and hence limits the applicability. Specifically when applied to different engine types such methods have to be reviewed, adapted or completely reconsidered.

In comparison to a broad scope of available diesel combustion modeling concepts, the complex dual fuel combustion problem has not been extensively investigated in the past. The reason might be associated to past emission legislation not being sufficiently stringent to make such concepts viable or economic aspects related to fuel price. Today, however, the need for modeling the dual fuel combustion is evident due to the increased interest in fuel-flexible operation and increasingly strict emissions limits. Pioneering work with respect to DF combustion modeling has been carried out by Liu and Karim [9] as they proposed a semi-empirical multi-zonal combustion model for full load performance and knock predictions. The model considers five individual zones describing the pilot spray regions, reacting zone and unburned gaseous zone. The heat release of the pilot combustion is described by two superposed Vibe functions and the ignition is determined by detailed kinetics. However, it does not involve models representing detailed physics of the combustion process, which must be considered critical for any application for engine performance optimization.

Summarizing the extensive literature study, there are at present no appropriate models or modeling methods for diesel and dual fuel combustion for large low speed 2-stroke marine engines meeting requirements for fast and sufficiently generic engine cycle simulation. Therefore, the demand to develop such a model for fast running engine performance analysis and optimization is indisputable. Moreover, the phenomenological aspects of uniflow scavenging,

peripheral diesel fuel injection with multiple injectors or direct gas admission in case of DF version require a novel approach considering the in-cylinder spatial differences in composition and temperature and model spray propagation.

3. Thesis Goals

Therefore, the scope and goals of the present work can be outlined as follows:

The main target of the present study is a comprehensive assessment of phenomenological aspects of combustion in large low speed uniflow scavenged 2-stroke marine engines and the identification of generally valid concepts for describing diesel and dual fuel combustion in such engines. This comprises the development of quasi-dimensional, physics-based and fast running combustion modeling methodology in order to enable engine performance analysis and optimization under both steady state and transient operation conditions.

Partial aims are related to the limitations of zero-dimensional concepts that can be eliminated by a quasi-dimensional modeling approach of phenomena that impact the model accuracy substantially. In particular, spray interactions for the diesel combustion model and gas admission and associated ignition delay in dual fuel operation are considered. In order to do so, multi-zone models have to be utilized for cylinder volume discretization, according to the respective needs of the diesel and DF combustion modes.

Validation of individual submodels is done preferably against experimental data, e.g. for diesel spray propagation and dispersion. The extensive research carried out in parallel on a spray combustion chamber (SCC) representative of the bore size, injector nozzle geometry and conditions specific for large 2-stroke marine diesel engines [3,4] has been instrumental in this context. However, due to the lack of specific experiments related to the respective phenomena, selected submodels need to be compared to multidimensional CFD simulation results. The final combustion models are validated against full scale engine data at various operating conditions and for different engine bore sizes. The number of engine type specific constants is intended to be minimized for the sake of generic model validity.

The models shall be integrated into the commercial 1D cycle simulation tool GT-Suite for both combustion scenarios by means of a user routine. In this way, a direct link between the routine and in-cylinder thermodynamics and engine performance can be established. Finally, the model capabilities for combustion prediction and engine performance optimization are to be demonstrated in case studies for transient engine loading and for integrated marine propulsion systems.

4. Diesel Model Formulation

The structure of the developed combustion model is outlined in *Figure 1*. Starting from the initial conditions in the combustion chamber at start of injection (SOI) and from the specific injection profile several paths are followed in the proposed model. Considering chronology, evaporation rate is governed by spray atomization in terms of droplet size distribution, temperature, fuel properties and entrainment rate of the oxidizer. These are directly related to thermodynamic in-cylinder conditions and turbulent flow field including swirl level. In parallel, ignition delay is calculated by means of an integral approach according to Stringer [17]. The fuel amount evaporated during the ignition delay is consumed in the premixed combustion phase. However, the main portion of fuel is burned in the following mixing controlled (diffusive) combustion phase.

In the latter, spray interactions that limit the local availability of the oxidizer and hence shape the final HRR are modeled by a quasi-dimensional spray interaction model.

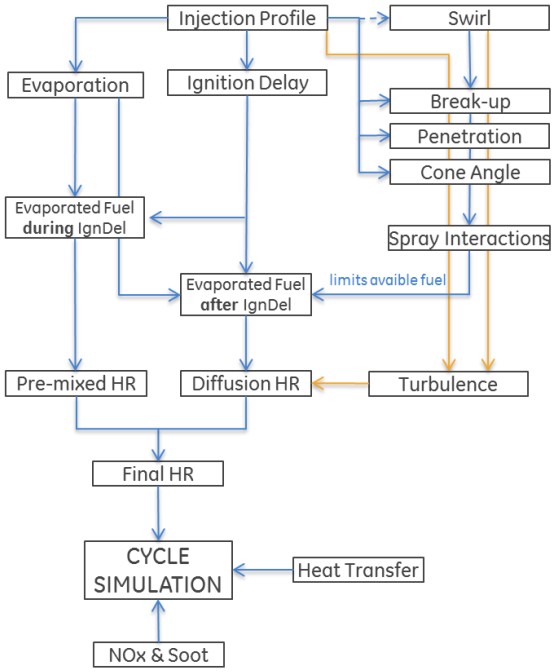

Figure 1 Schematic structure of the proposed diesel combustion model

The morphology of diesel spray is determinative in terms of fuel atomization, mixing with oxidizer and evaporation progress. Therefore, understanding the spray formation in detail becomes essential for a generic burn rate prediction. The spray formation process initiated by the liquid fuel entering the combustion chamber at high velocity comprises several phases. The primary break-up is characterized by the disintegration of spray ligaments into large droplets induced by turbulence and cavitation effects. The secondary break-up is generally driven by aerodynamic stripping of smaller droplets from larger droplets or disintegration of larger droplets due to the effect of normal stresses.

Spray penetration

Various concepts quantifying the spray tip penetration of liquid fuel injected directly in the cylinder are found in literature. Selected correlations were validated against experimental results from the SCC. It has been shown that existing correlations underestimate spray propagation both prior to and after the liquid core break-up. To match the experimental observations with better accuracy, an adapted correlation was proposed by von Rotz et al. [4]. This approach takes specifics of large 2-stroke marine engines in respect of injector position, nozzle geometry, fuel quality, in-cylinder temperature and pressure level as well as typical swirl motion into account. As demonstrated in *Figure 2*, the agreement with the experiments was improved substantially when comparing to correlations available in literature.

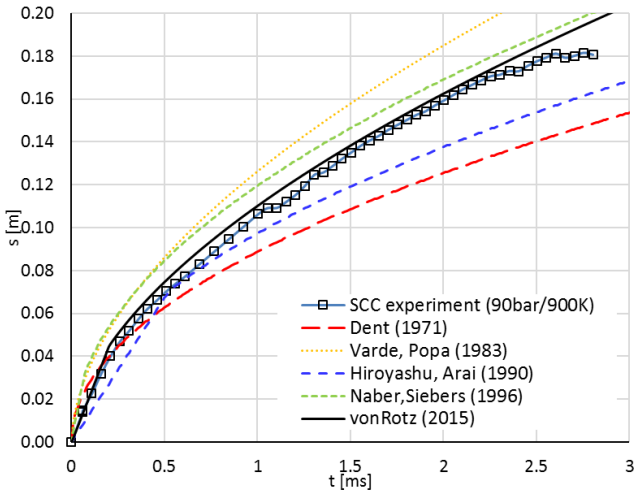

Figure 2 Experimental and correlated spray tip penetration at 900K, 90bar and 1000bar rail pressure

Analogous to the approach of Hiroyasu and Arai [7], the spray tip penetration is defined by separate correlations prior to and after spray breakup time. For the region close to the nozzle hole exit, the spray velocity is calculated according to the Bernoulli equation and proportional to the ratio of the gas density and the reference air density following equation (1).

$$s\,(t < t_{br}) = 1.16\left(\frac{2\Delta p}{\rho_f}\right)^{0.5}\left(\frac{\rho_g}{\rho_{air}}\right)^{-0.22} t \tag{1}$$

After the transition to the post spray breakup phase the ratio of effective injection pressure and density of ambient gas in the combustion chamber determines spray penetration as initially proposed in [7]. Furthermore, introduction of a dependency on gas temperature and the nozzle hole diameter according to [4] yields equation (2).

$$s\,(t \geq t_{br}) = {T_g}^{-0.2}{\rho_f}^{0.15}\left(\frac{\Delta p}{\rho_g}\right)^{0.28}{d_{noz}}^{0.35}\,t^{0.56} \tag{2}$$

The spray breakup time t_{br} is defined by the concurrence of both spray penetration before and after transition phase from liquid jet to gas entrainment evolution according to [7].

$$t_{br} = 28.65\,\frac{\rho_f d_{noz}}{\sqrt{\rho_g \Delta p}} \tag{3}$$

Spray dispersion

A common way of describing spray dispersion is by defining the cone angle of its outer boundaries, in line with results from experimental observations. Using the shadow-imaging technique with back illumination allows capturing spray evolution even after the ignition process is terminated. In this way, valuable information about spray evolution could be obtained from the experiments in the SCC [3,4]. For the phenomenological model, reactive evaporating conditions are considered as relevant for real engine operation. Compared to nonevaporating conditions, in the reactive case the spray angle contraction is caused by the cooling effect of fuel evaporation on the entrained gas. Experimental SCC results in terms of spray contour with nozzle hole diameter of 0.875mm and 1000bar rail pressure are used for validation.

Several correlations proposed in the past were evaluated at various conditions and compared with data from measurements after spray stabilization. Since these correlations are mainly based on investigations utilizing small nozzle diameters and thus not comparable with dimensions used in large marine engines, they tend to overestimate spray dispersion at those conditions. Investigations carried out on the SCC have confirmed the dependency of the spray cone angle on the ratio of the ambient gas and fuel densities whereas the impact of nozzle diameter and injection pressure on the spray dispersion was minor [4]. These observations are in alignment with conclusions made by Naber and Siebers [10]. Nevertheless, the exponential coefficient of the densities ratio in equation (4) was tuned to fit experimental results.

$$tan\left(\frac{\theta}{2}\right) = \frac{1}{4}\left(\frac{\rho_g}{\rho_l}\right)^{0.24} \tag{4}$$

Evaporation

Spray atomization process is predominant in terms of ensuing droplet heating and evaporation related to the phase transition of the injected liquid fuel to vapor. Without consideration of the droplet coalescence, the initial liquid blob gradually breaks up into smaller drops and eventually evaporates. For the present application, significant simplifications have been made assuming spherical and symmetrical single-phase droplets with constant density and pressure. Further, impact of radiation, kinetics, semi-transparency of droplets, vapor superheating and droplet internal turbulence are neglected. Hence, the main driver of the droplet heating and evaporation is attributed to both diffusion and convection. Adopting the classical Spalding hydrodynamic model concept [11], the rate of droplet evaporation is determined by relation (5) where the density ρ_f and diffusion coefficient D_f are related to the fuel vapor, r_{dr} represents the instantaneous droplet diameter initiated by Sauter mean diameter (SMD), determined by means of a correlation proposed by Varde [12]. *Sh* denotes Sherwood number and B_M Spalding mass transfer number.

$$\frac{dm_{dr}}{dt} = 2\pi\, D_f\, \rho_f\, r_{dr}\, Sh\, B_M \tag{5}$$

Based on the change of the droplet mass transfer rate given by equation (6) the droplet diameter can be determined according to Faeth [13].

$$\frac{dr_{dr}}{dt} = \frac{1}{4\pi \cdot {r_{dr}}^2 \rho_f}\frac{dm_{dr}}{dt} - \frac{r_{dr}}{3\rho_f}\frac{d\rho_f}{dt} \tag{6}$$

Turbulence Model

In terms of simplified zero-dimensional turbulence modeling, the turbulent kinetic energy is to be addressed as the specific kinetic energy of the mean flow field. Fundamentally, this implies resolution of two main characteristic quantities, integral length scale l_I and turbulence intensity *u'*. For piston engine relevant problems, the integral length scale can be determined according to [2] on the basis of instantaneous cylinder volume, thus accounting for variable density. Under assumption of system isotropy and homogeneity the turbulence intensity can be determined from equation (7)

$$u' = \sqrt{\frac{2}{3}k} \tag{7}$$

To estimate the turbulence intensity *u'* a simplified zero-dimensional turbulence model is derived following past efforts successfully applied for resolving turbulence in reciprocating engines [11,12]. The proposed turbulence model relies on the *k-ε* formulation adopting the concept of the energy cascade having its origin in the largest scale eddies. Merely the largest scale determined from the mean kinetic energy is resolved. Hence, production terms of the turbulent kinetic energy can be assigned to major source terms and designated as kinetic energy of the main flow field. Specifically, kinetic energy of the injection spray, density variations and swirl motion are considered relevant production source terms in the present model. The rate of change of the turbulent kinetic energy *k* (TKE) is defined as the sum of turbulence source terms and its dissipation rate ε, defined by equation (8).

$$\frac{dk}{dt} = \left(\frac{dk}{dt}\right)_{density} + \left(\frac{dk}{dt}\right)_{swirl} + \left(\frac{dk}{dt}\right)_{inj} - \varepsilon \tag{8}$$

As consequence of the cyclic engine piston stroke the production term based on compressibility effects influencing the viscosity and Reynolds number is related to in-cylinder density changes by equation (9) as proposed in [16].

$$\left(\frac{dk}{dt}\right)_{density} = \frac{3}{2} k \frac{1}{\rho} \frac{d\rho}{dt} \tag{9}$$

For the formulation of the phenomenological combustion model the kinetic energy arising from the direct fuel injection is of major importance since it directly impacts the turbulent mixing and fuel oxidation progress. This is modelled by means of a rather simple approach for determining the kinetic energy of the fuel spray from the injection velocity defined by the Bernoulli equation and corresponding discharge coefficient. Analogous to [16], the specific kinetic energy of fuel injection can be obtained by relating the kinetic energy to the total in-cylinder mass following equation (10).

$$\left(\frac{dk}{dt}\right)_{inj} = \frac{1}{2} \frac{dm_{inj}}{dt} u_{inj}^2 \frac{1}{m_{cyl}} \tag{10}$$

The effect of swirling flow on turbulence production is related to the radial distribution of angular momentum in the cylinder and hence the production term is directly linked to the mass flow rate through inlet ports and tangential velocity u_{tan} according to equation (11)

$$\left(\frac{dk}{dt}\right)_{swirl} = C_{swirl} \cdot \frac{1}{2} \frac{dm_{IP}}{dt} u_{tan}^2 \frac{1}{m_{cyl}} \tag{11}$$

Finally, the dissipation rate is defined proportionality to the turbulence intensity and the integral length scale. Transforming the turbulence intensity to the turbulent kinetic energy for zero-dimensional isotropic conditions the turbulence dissipation is defined by (12).

$$\varepsilon \sim \frac{u'^3}{l_I} = \frac{1}{l_I} k^{3/2} \tag{12}$$

The integral length scale is determined from the instantaneous cylinder volume as the diameter of the equivalent sphere as defined by equation (13)

$$l_I = \left(\frac{6 \cdot V_{cyl}}{\pi}\right)^{1/3} \tag{13}$$

The model constants of individual turbulent kinetic energy source terms were tuned to match averaged turbulent kinetic energy (TKE) profiles calculated by means of CFD at various engine loads. For this purpose, the user combustion model was implemented in a 1D cycle simulation and TKE history was tracked during the scavenging phase from inlet port opening (IPO) at 144.5

DATDC until termination of the combustion as shown on *Figure 3*. Comparing the detailed CFD results with the simplified turbulence model on the left, good agreement throughout the entire engine cycle is achieved. Several minor differences are worth noting and briefly discussed: Besides an early phase difference arising from boundaries mismatch, flow pattern and timestep resolution there is a slight overestimation in the compression phase. On the other hand, as regards TKE determination during the combustion phase, where the calculated burn rate is governed by the turbulent mixing process, the reduced model shows good fidelity.

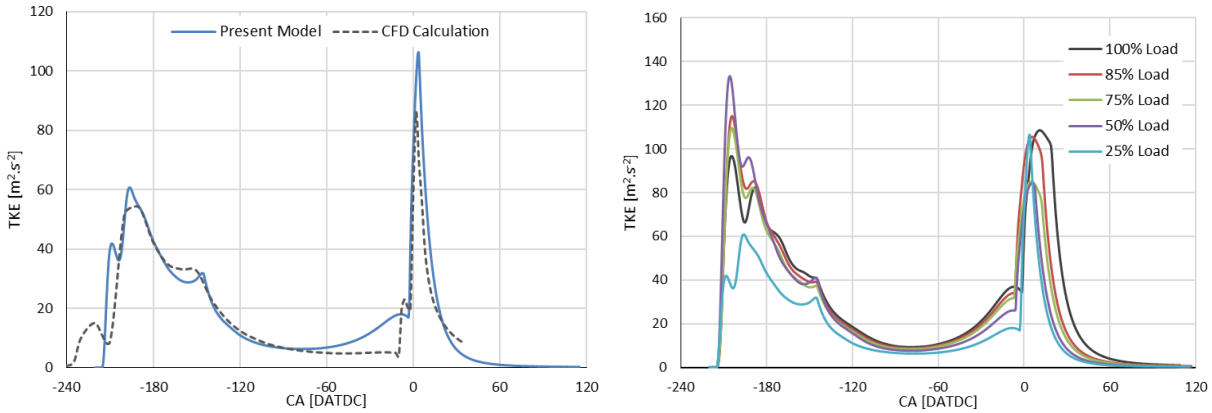

Figure 3 Turbulence model results compared with cylinder averaged TKE calculated by means of CFD (left), simulated TKE for load variation of RT-flex60 engine (right)

Employing the proposed turbulence model for engine cycle simulations for a load variation along the propeller curve, the resulting crank angle resolved history of the turbulent kinetic energy can be plotted as shown on the right in *Figure 3*. Apparently, for all engine loads the turbulence generated by the intake port swirling flow largely dissipates during the compression phase. Hence, any differences in the TKE level depending on engine load prior to injection onset are not determinative. The turbulent mixing is primarily controlled by the fuel injection turbulence source.

Ignition and Premixed Combustion

Ignition of the fuel spray defines the onset of the energy release and thus needs to be determined precisely. Essentially, the ignition delay is described by the time elapsed between start of injection and the occurrence of OH radicals and involves both physical and chemical processes. The ignition delay duration depends on engine operating conditions, injection pressure, fuel quality, injector and nozzle geometry as well as on a wide range of chemical reactions characterized by various temperature regimes and time scales. Commonly employed correlations assume an averaged ignition delay linked to a global reaction involving all intermediate steps and states of individual processes. Such approximation can be also justified for the present model since the ignition delay compared to the combustion duration is negligible. Hence, a simplified empirical approach is implemented in form of Livengood-Wu integral, in which the immediate ignition time is determined as a function of in-cylinder pressure and temperature history according to Stringer [17].

$$\tau_{ign} = C_{ign}\, p^{-0.75} e^{\left(\frac{5473}{T}\right)} \tag{14}$$

Typically, for today's efficiency-optimized 2-stroke marine diesel applications the premixed combustion is negligible. However, for DF engine applications with low compression ratio it becomes more pronounced and needs to be considered in the modeling approach. In the present work, a concept relying on the characteristic premixed time scale τ_{ign} is employed following the approach defined in [15]. The ignition delay period is decisive in terms of fuel amount prepared to be directly oxidized immediately after combustion start. The fuel burned within the premixed

combustion model is defined as the fraction evaporated during the ignition delay according to equation (15), where $m_{f,u,prem}$ denotes unburned fuel evaporated during the ignition delay and available for premixed combustion.

$$\frac{dm_{f,b,prem}}{dt} = C_{prem}\frac{1}{\tau_{ign}}m_{f,u,prem} \tag{15}$$

Diffusion Combustion

After the evaporated fuel during the ignition delay has been oxidized the major part of the injected fuel is converted in the diffusion combustion mode. The diffusion burning of evaporated and mixed fuel that is allocated within a region with sufficient oxygen availability is defined by the time scale approach. Adopting the time scale model concept introduced by Weisser [15] the reaction rate is calculated using the corresponding turbulent time scale analogous to eddy break-up models often employed in CFD codes. The mixing controlled oxidation is governed predominantly by turbulence whereas kinetics is not dominant. The diffusion burn rate is formulated based on the turbulent time scale τ_T and the available evaporated unburned fuel $m_{f,un,diff}$.

$$\frac{dm_{f,b,diff}}{dt} = C_{diff}\frac{1}{\tau_T}m_{f,u,diff} \tag{16}$$

The turbulent time scale is essentially determined by the structure of the turbulent flow field. For the simplified 0D model an approximation related to the turbulent viscosity $u'l_I$ and a characteristic diffusion length scale l_{diff} is used and the turbulent mixing frequency is determined according to equation (17).

$$\frac{1}{\tau_T} = \frac{u' l_I}{l_{diff}^2} \tag{17}$$

The characteristic length scale of relevance here is assigned to the largest eddies in the flow that are predominant in terms of momentum and energy transport. This diffusion length scale l_{diff} is derived from the mixing length of fuel and oxidizer and is associated with a characteristic dimension of the system. Here, the volume-to-surface ratio of the cylinder volume and the total fuel spray area is used. The total fuel spray area is defined as the sum of all individual spray areas resulting from spray penetration and interaction. After the injection of fuel is terminated, the spray area is set to a constant equal to its value at EOI.

$$l_{diff} = \frac{V_{cyl}}{A_{fl,tot}} \tag{18}$$

Spray Interactions

Due to design constraints and to ensure proper fuel distribution and atomization within the entire combustion space large 2-stroke diesel engines require multiple injectors. Depending on engine size the combustion space accommodates two or three circumferentially located injectors. The resulting burn rate is determined primarily by the fuel injection profile and the turbulent mixing process controlling the diffusion combustion. In addition, interactions among individual sprays retard the combustion progress as the unburned fuel enters areas with burned gas originating from the injector located upstream with respect to swirl motion. The local lack of oxidizer leads to burn rate deceleration followed by a recovering phase as the unburned fuel is transported into regions of more favorable oxidizer concentration.

In this respect, a zero-dimensional modelling approach is not sufficient to capture spray interaction effects. Therefore, a quasi-dimensional discretization of the spray is proposed to

account for spray interactions that impact the combustion progress. The in-cylinder swirl profile in terms of tangential flow velocity u_{tan} is characterized by a polynomial formula (19) based on work of Nakagawa [18].

$$u_{tan} = u_{tan,max}\left[C_1\left(\frac{r}{r_{tot}}\right) + C_2\left(\frac{r}{r_{tot}}\right)^2 + C_3\left(\frac{r}{r_{tot}}\right)^3\right] \tag{19}$$

Coefficients C_1, C_2 and C_3 are determined by matching the calculated swirl profile with CFD results according the *Figure 4*. In case of confined swirl, the tangential velocity increases proportionally with radius until it is damped in the wall boundary layer and ultimately reaches zero at the wall.

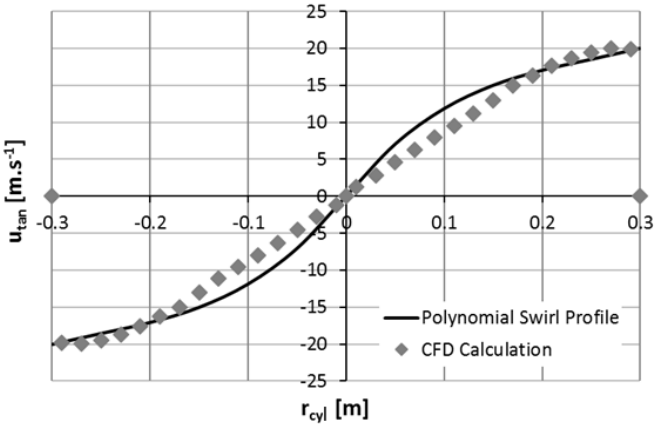

Figure 4 Polynomial swirl profile plotted over cylinder radius r_{cyl} and compared with CFD results for full load conditions of RT-flex60 engine

Spray morphology is characterized by correlations validated against SCC experiments described by equations (1-4). Tip penetration and dispersion angle are tracked for each single nozzle hole considering the actual nozzle geometry, injection strategy, fuel properties and in-cylinder conditions. The instantaneous spray velocity is determined by the resulting undisturbed penetration speed and the swirl level at the actual spray position. Considering the difference in momentum of the fuel and the entrained air, the initial tangential velocity defined by the swirl profile is corrected by the mass ratio at the current time step. Employment of the momentum conservation yields the relation for the entrainment air mass (20) where $u_{f,0}$ is the fuel velocity at the nozzle exit.

$$m_{air} = m_f\left(\frac{u_{f,0}}{u_f} - 1\right) \tag{20}$$

The deflection velocity changes the spray trajectory based on initial velocity, swirl profile and air entrainment rate. The model constant C_{defl} determines to what extent the direction of the penetrating spray is affected by the in-cylinder swirl in respect of the entrained air mass.

$$u_{defl} = C_{defl}\left(\frac{m_a}{m_{air} + m_f}\right)u_{tan} \tag{21}$$

The final spray velocity u_{spray} is the product of a vector addition of the initial spray tip velocity from the previous time step and the deflection velocity determined from the in-cylinder swirl profile at the actual position of the spray tip and the impact of momentum conservation. The instantaneous position of each individual spray tip at time step *i* is calculated in form of mathematical formulas for *x, y* and *z* coordinates originating at the location of the respective injector. Depending on nozzle hole vertical *(α)* and horizontal *(β)* angles penetration increment and actual deflection velocity, the spray position is calculated based on its location at previous step i-1 according to definition in (22-24).

$$x_i = x_{i-1} + \cos\beta(s_i - s_{i-1}) + \sin\left(atan\left(\frac{y_{i-1}}{r_{inj} - x_{i-1}}\right)\right) u_{defl} \cdot dt \tag{22}$$

$$y_i = y_{i-1} + \sin\beta(s_i - s_{i-1}) + \cos\left(atan\left(\frac{y_{i-1}}{r_{inj} - x_{i-1}}\right)\right) u_{defl} \cdot dt \tag{23}$$

$$z_i = z_{i-1} + \frac{\sqrt{(x_i - x_{i-1})^2 + (y_i - y_{i-1})^2}}{\tan\alpha} + \cos\left(atan\left(\frac{y_{i-1}}{r_{inj} - x_{i-1}}\right)\right) u_{defl} \cdot dt \tag{24}$$

Graphical interpretation of the quasi-dimensional spray penetration within the combustion space is presented in *Figure 5* on the left. Here, the case of co-swirl injection with three peripheral injectors is considered. The initial spray tip velocity and direction at the nozzle outlet are calculated based on the instantaneous injection pressure and injector geometry, respectively. In dependence on in-cylinder conditions and the swirl profile the spray is deflected. At each time step the resulting spray velocity vector u_{spray} is determined based on its value from previous step $u_{spray,0}$ and the deflection velocity resulting from the momentum balance equation (18). The penetration progress for individual sprays at the spray interaction onset is shown in *Figure 5* on the right.

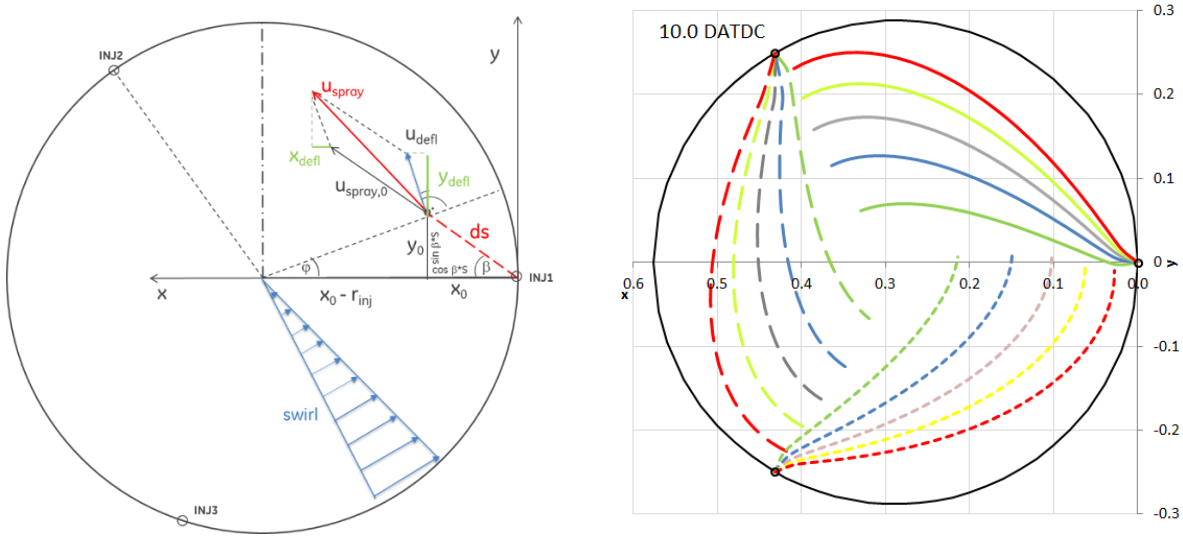

Figure 5 Geometrical interpretation of the quasi-dimensional spray interaction model and temporal penetration progress for individual sprays for RT-flex60 engine at nominal load and 800bar fuel rail-pressure.

The two-dimensional resolution of the cylinder aiming to track the spray penetration history is completed by a 3D model of individual sprays in the form of a hemispherical spray front and an attached cone representing the spray body. The area of an individual spray is determined by (25) from the spray penetration length s and the radius of the spray tip r_{tip} calculated based on the spray dispersion angle (4).

$$A_{spray} = 2\pi \cdot r_{tip} + \pi \cdot r_{tip}\left(r_{tip} + \sqrt{{r_{tip}}^2 + (s - r_{tip})^2}\right) \tag{25}$$

The ratio of spray area interacting with burned gases from the upstream injector to the total area determines the available evaporated fuel that can be burned in actual time step. Following this

concept, the unburned fuel available for the diffusion combustion is given by equation (26). Index *j* identifies particular nozzle hole and n denotes the total number of injector holes.

$$m_{f,u,diff} = m_{f,u,evap} \frac{\sum_{j=1}^{n}\left(A_{spray,j} - A_{spray,interact,j}\right)}{\sum_{j=1}^{n} A_{spray,j}} \tag{26}$$

5. Dual Fuel Model

Dual fuel combustion is distinguished by a high level of complexity related to deviations from stoichiometric and homogenous conditions. A good level of understanding of individual phases is required to derive a simplified modeling approach which is comprehensive enough to capture the physics appropriately. Hence, extensive computational and experimental investigations were evaluated to identify major mechanisms governing mixing process, ignition delay and turbulent flame propagation. *Figure 6* illustrates the schematic structure of the dual fuel combustion model developed for the 2-stroke lean burn gas engine. The blue arrays characterize the immediate computational sequence and the red lines denote feedback links. First of all, the thermodynamic state together with instantaneus equivalence ratio and cylinder flow field are substantial with respect to the premixed combustion process. Fuel oxidation is governed by correlations for both laminar and turbulent flame velocities. It is also worth noting that the second feed back path is associated with the pilot heat relase rate calculation that defines the global combustion onset in case combustion is not initiated by selfignition. According to the diagram, the model features a large number of submodels associated to gas admission, pilot fuel injection, ignition delay for both pilot and main fuels, laminar and turbulent flame velocities correlations and finally the resulting global heat release rate.

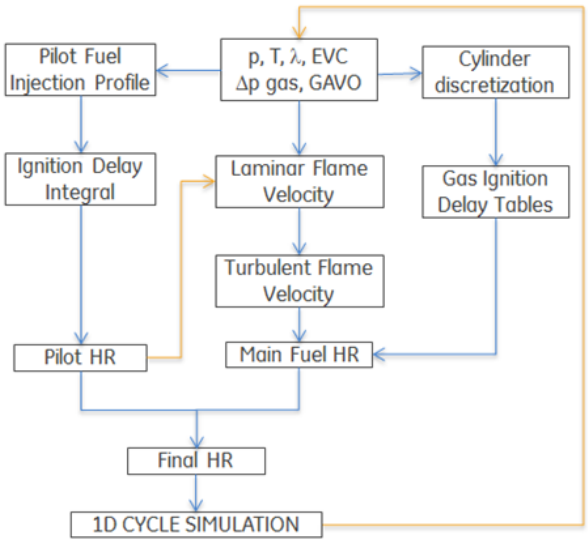

Figure 6 Schematic of the dual fuel combustion model structure

The transition from the flame front propagation into the actual burn rate is done by assuming a spherical penetration of the turbulent flame front originating from the pilot flame jet as described in the following section. The swirl motion induced by the inlet ports and further enhanced by the co-swirl gas admission is beneficial both for improving the mixing of reactants and to secure highest possible combustion efficiency by steering the flame propagation in the favorable way. This effect is further enhanced by pointing the outlet of the pilot combustion chamber (PCC) in

the flow swirl direction. The combustion chamber accommodates two opposite PCCs located on the circumference as schematically illustrated in *Figure 7*. For the sake of simplicity essential for fast running model application, the progress of dual fuel combustion is characterized by pilot fuel injection into the PCC, burning jet penetration into the main combustion space, ignition of the main gaseous fuel mixed with oxidizer and the resulting flame front propagation through the main combustion chamber.

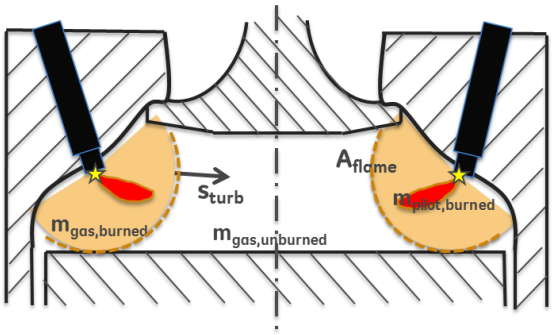

Figure 7 Schematic representation of the combustion chamber and the flame front propagation

For the dual fuel combustion model the ignition delay is determined for both liquid and gaseous fuel individualy. Under normal conditions, the combustion start is triggered solely by pilot injection timing. Hence, burn rate calculation depends on the flame front propagation defined by premixed flame turbulent velocity, flame front area, unburned zone conditions as well as combustion progress variable according to equation (27).

$$\frac{dm_b}{dt} = \frac{\rho_u}{1 + \frac{1}{\phi} \cdot AFR_{st}} S_T \cdot A_{fl} \tag{27}$$

The theoretical flame area correlation relies on the simplified spherical flame front propagation induced by the pilot fuel combustion start. In fact, hemispherical flame flont propagation is assumed in view of the combustion chamber geometrical boundaries, pilot jet inclination and swirl direction, according to expression (28), where r_{fl} denotes flame radius and x_b is the burn rate progress variable.

$$A_{fl} = 4 \cdot \pi \cdot r_{fl}^2 \frac{1}{12} \cdot (1 - x_b) \tag{28}$$

Pilot Fuel Combustion

In large low speed 2-stroke DF engines the pilot fuel energy content corresponds to merely around 1% of the total fuel energy input. Elevated temperature levels in the PCC throughout the entire cycle lead to insignificant ignition delay at all operating conditions. Hence, the ignition delay of the pilot fuel can be approximated empirically by using a Livengood-Wu type correlation without introducing any major discrepancy to the model. The combustion rate is calculated by adopting the time scale approach according to [15] following equation (29).

$$\frac{dm_{f,b,pilot}}{dt} = C \frac{u'}{l_{PCC}} m_{f,u} \tag{29}$$

The characteristic length scale l_{PCC} is related to the PCC volume and the turbulence intensity is calculated analogical to the approach defined for the diesel model, with TKE determined according to equation (6). However, in the case of pilot combustion merely the turbulence source term arising from pilot fuel injection kinetic energy and dissipation are considered.

Figure 8 represents pilot fuel injection rate profile, TKE progress and the resulting integrated burn rate for full load operation of the RT-flex50DF engine. The model was calibrated against measured pressure profiles in the PCC without partial validation of the submodels, e.g. for TKE. From *Figure 8* it can be concluded that the pilot fuel combustion progresses rapidly and the majority of the injected fuel is burned already within the injection phase.

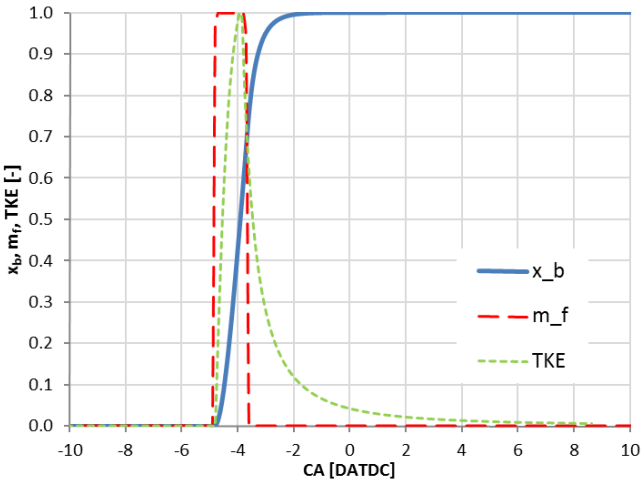

Figure 8 Integrated pilot fuel burn rate and corresponding non-dimensional injection rate and TKE

Gas Ignition Delay

Employing an ignition delay mechanism linked to the mean thermodynamic conditions of the unburned zone for calculations of various engine types has shown a significant discrepancy between simulation and experimental results. Hence, it is obvious that the ignition delay determination based on the average temperature is not applicable for capturing the real engine operation. Local temperature gradients and gas concentration variations play an important role during the ignition delay phase, especially when rich mixture directly interacts with the high temperature zone originating from hot rest gases located mainly below exhaust valve. This leads to a considerable reduction of ignition delay characterized by advanced occurrence of combustion start and introduces a discrepancy into the ignition prediction.

To capture spatial variations within the cylinder, a discretization methodology is proposed that accounts for the local variation of burned fraction, temperature and gas concentrations. Schematics of the vertical discretization method is illustrated in *Figure 9*. The total cylinder volume is equally divided into a user specified number of sub-volumes, i.e. zones. For each zone the burned and unburned mass fractions are calculated according to instantaneous mass flows at inlet ports and exhaust valve determined directly during a 1D cycle simulation from the engine model. Governing equations for mass and energy conservation are formulated according to Macek [19] by equations (30) and (31), respectively.

$$\frac{dm_i}{dt} = \sum_{i=0}^{n} \frac{dV_i}{dt}\left(\rho_{i-1} w_{i-1,i} - \rho_{i+1} w_{i,i+1}\right) + \dot{m}_{in} - \dot{m}_{exh} + \dot{m}_g \tag{30}$$

$$\frac{d(m_i h_i)}{dt} = \sum_{i=0}^{n} \frac{dV_i}{dt}\left(h_{i-1}\rho_{i-1} w_{i-1,i} - h_{i+1}\rho_{i+1} w_{i,i+1}\right) + m_i\left(h_{i-1} w_{i-1,i} - h_{i+1} w_{i,i+1}\right) + \alpha_Q A_i (T_{wall} - T_i) + V_i \frac{dp_i}{dt} \tag{31}$$

Mass fluxes are related to intake, exhaust and gas flows and become valid for relevant zones only. Instantaneous transfer of burned gas and fresh air is computed between adjacent zones and defines the burned mass fraction at the end of every time step. This is then determinative for the amount of transferred burned and fresh gas within the following time step. Perfect mixing is assumed so that the zonal temperature is defined by the burned mass fraction and the temperatures of both unburned and burned gases. Additional increase of zonal temperature is due to the heat transfer from the wall which involves an empirical correlation for liner temperature distribution.

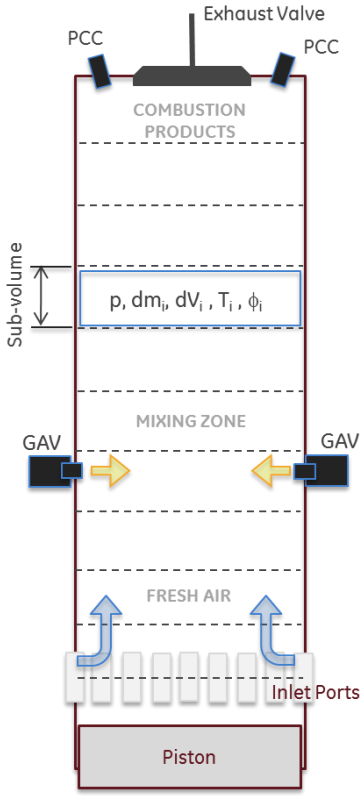

Figure 9 Schematics of cylinder volume discretization

Laminar Flame Speed

The approach adopting a polynomial function developed for lean conditions by Witt and Griebel [20] was used as a basis for deriving a correlation determining the laminar flame front velocity, defined by equations (32-34). As stated above, the equations have been adjusted to ensure accurate response under relevant engine operation conditions. In particular, the pressure dependency of the constant C_2 in equation (34) was tuned in order to fit the detailed kinetics computation results [16].

$$s_L = C_1 \cdot p_{cyl}^{-C_2} \tag{32}$$

$$\begin{aligned} C_1 = {} & (-6.906 \cdot 10^{-5}\, T_{un}^2 + 0.06875\, T_{un} - 25.13)\phi^3 \\ & + (1.155 \cdot 10^{-4}\, T_{un}^2 - 0.11523\, T_{un} + 46.47)\phi^2 \\ & + (-4.185 \cdot 10^{-5}\, T_{un}^2 + 0.04922\, T_{un} - 24.82)\phi \\ & + (6.57 \cdot 10^{-6}\, T_{un}^2 - 9.55 \cdot 10^{-3} T_{un} + 5.185) \end{aligned} \tag{33}$$

$$C_2 = \left(\frac{1}{2\, p_{cyl}}\right)^{-0.25} \tag{34}$$

The predictivity of this laminar flame speed correlation is assessed by applying a detailed reaction mechanism [21] for eight selected cases relevant to real engine operation. *Table 1* summarizes initial conditions for considered cases in terms of temperature, pressure and equivalence ratio. Laminar flame velocity for both detailed mechanism and the present model are visualized in *Figure 10*. Apparently, for the selected cases the agreement between the detailed mechanism and the adopted correlation is on a very good level. Nevertheless, it is worth noting that based on this comparison no general statement about the accuracy of the phenomenological model can be made since the spatial inhomogeneity and the impact of turbulence are also essential.

case	1	2	3	4	5	6	7	8
p [bar]	50	50	50	50	50	100	120	140
T [K]	800	1000	800	800	1000	850	975	625
ϕ	0.5	0.5	0.75	1.0	1.0	1.0	0.7	1.4

Table 1 Overview of validation cases for the laminar flame velocity at engine relevant conditions corresponding to the *Figure 10*

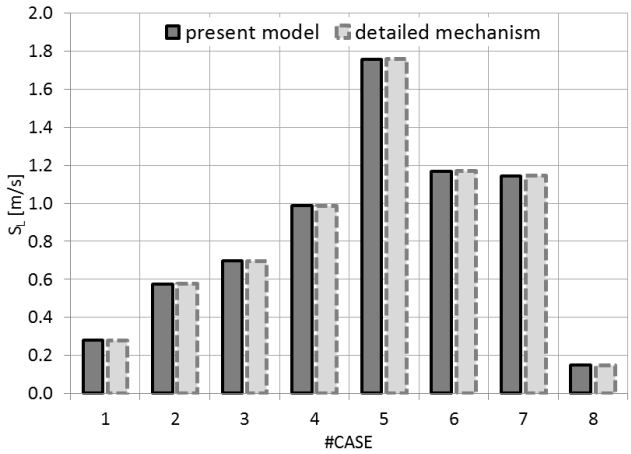

Figure 10 Validation cases relevant for engine operation defined by *Table 1* showing comparison of laminar burning velocities determined by the present model and detailed kinetics mechanism [21]

Turbulence Model

Turbulence production in a large 2-stroke DF engine is governed primarily by the swirling flow field generated during the scavenging process, admission of the gaseous fuel and the compressibility linked to the density changes as a consequence of piston motion. Note that injection of the pilot fuel was incorporated merely for modeling pilot fuel combustion in the PCC. Parallel to the approach employed for the diesel model turbulence generated by the combustion itself is not taken into account. This is valid for both pilot and main gaseous fuels. Consideration of all major turbulence source terms for dual fuel operation results in the general formula (35). The density change is represented by the first term on the right side. The second term stands for the increase of the specific kinetic energy generated by the admission process of the gaseous fuel into the cylinder. Finally, the dissipation term is defined in accordance with formula (12), with the integral length scale determined by the physical flow boundaries, in this case defined by the PCC volume (36) analogous to [16].

$$\frac{dk}{dt} = \frac{3}{2}k\frac{1}{\rho}\frac{d\rho}{dt} + \frac{1}{2}\frac{dm_g}{dt}u_g^2\frac{1}{m_{cyl}} - C_{diss}\cdot\frac{1}{l_I}k^{\frac{3}{2}} \tag{35}$$

$$l_I = \left(\frac{6\,V_{PCC}}{\pi}\right)^{1/3} \tag{36}$$

The instantaneous gas flow is calculated using a flow function for compressible conditions following equation (37), where A_{GAV} denotes effective gas nozzle area and C_D discharge coefficient.

$$\frac{dm_g}{dt} = C_d A_{GAV}\sqrt{2\rho_g p_g\left(\frac{\kappa}{\kappa-1}\right)\left[\left(\frac{p_{cyl}}{p_g}\right)^{\frac{2}{\kappa}} - \left(\frac{p_{cyl}}{p_g}\right)^{\frac{\kappa+1}{\kappa}}\right]} \tag{37}$$

To determine gas density relevant for conditions at the GAV nozzle outlet actual admission pressure and temperature are included in formula (38) with compressibility factor Z= 0.988 for methane.

$$\rho_g = \frac{p_g M_{CH4}}{T_g R\, Z} \tag{38}$$

The initial value of the kinetic energy k_{ini} is determined by the swirl level which in turn depends on the intake flow velocities according to equation (39). It is worth noting that based on findings from the zero-dimensional turbulence model for diesel combustion an explicit determination of the swirl governed turbulence source term is omitted.

$$k_{ini} = C_k\frac{1}{2}u_{IP}^2 \tag{39}$$

Figure 11 illustrates the calculated turbulent kinetic energy *k* for full load and 25% load case compared against CFD results averaged over the entire combustion chamber. Gas mass flow rate profiles correspond to the calculated model input based on effective gas pressure and GAV nozzle geometry.

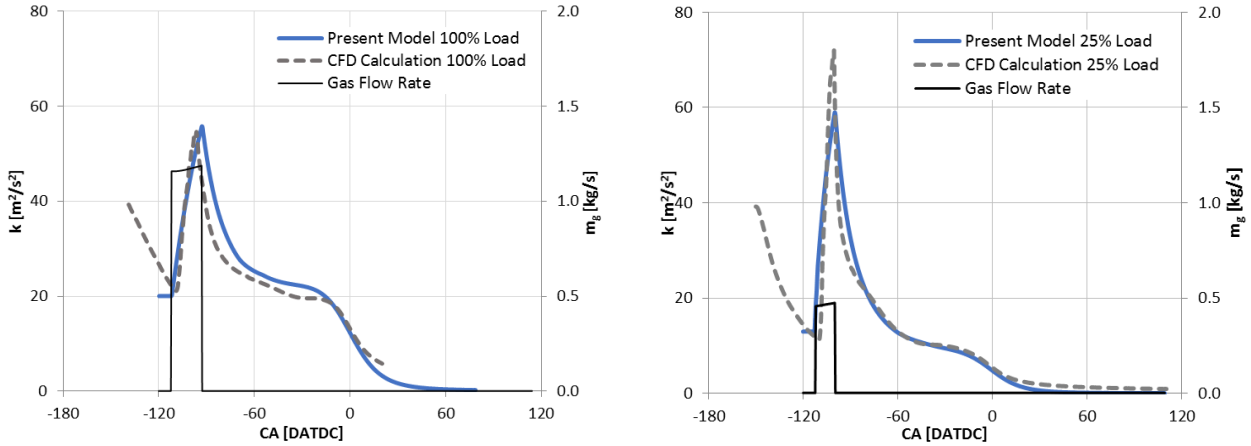

Figure 11 Calculated turbulent kinetic energy profile compared with CFD averaged results at 100% and 25% engine load operation

Obviously, gas admisson is the predominant turbulence source term within the period in question and can be expected to vary as a function of load. Note that the impact of the GAV nozzles orientation is not modeled due to limited availability of CFD data for validation. Any turbulence generated by the combustion process itself is also not considered in the present model. However, this effect is partly taken into account through the turbulent flame velocity definition dicussed in the following section.

Turbulent Flame Speed

Based on the analogy with laminar flame propagation, the turbulent flame velocity can be determined. Turbulent effects caused by the oxidation process itself act direcly on the flame and hence the theoretical turbulent flame velocity cannot be the only measure of the oxidation rate [22]. Therefore, the influence of flame stretch must be considered. Eventhough aquiring experimental data becomes progressively challenging as the turbulence level increases, meanwhile computational studies help to reveal the effect of flame strech on turbulent flame velocity [22,23]. Nevertheless, for quasi-dimensional phenomenological models such effect cannot be captured in detail and a strong simplification is often inevitable.

Identifying the combustion regime for the present case helps to gain a better understanding of the fundamental processes and thus select a suitable computational method. Therefore, various load points are investigated by means of premixed turbulent flames classification within a regime diagram in order to interpret the turbulence impact on combustion correctly. The relevant parameters related to the mixture and flow field properties are laminar flame velocity S_L, turbulence intensity u', integral length scale l_I and reaction zone thickness. These variables are expressed in a form of nondimensional numbers, in particular Damköhler number *Da*, Karlovitz number *Ka* and turbulent Reynolds number Re_T. Assuming homogenous and isotropic turbulence, these nondimensional numbers can be used to determine the predominant combustion regime according to the classification proposed by Peters [18]. Selected DF engine operation points can then be visualized in the regimes diagram for premixed turbulent flame as shown in *Figure 12*.

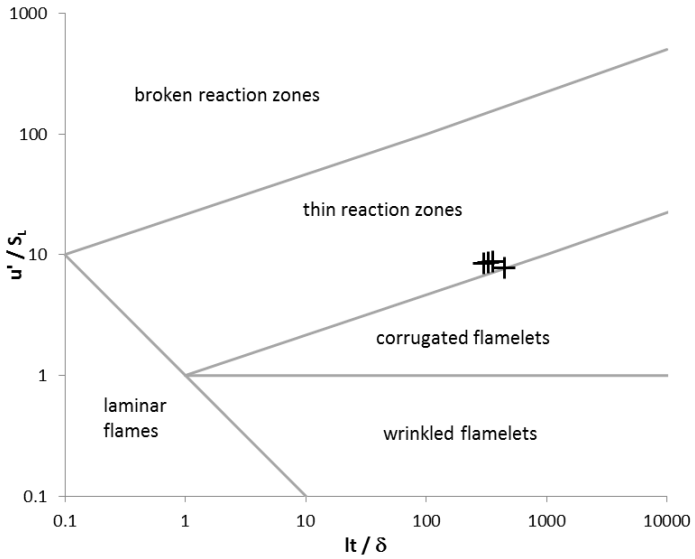

Figure 12 Regime diagram according to Peters [23] showing experimental points from Table 2

Table 2 summarizes main parameters related to turbulent flame at four different engine loads corresponding to the *Figure 12*. The conditions are considered prior to combustion start at a temperature level of about 800K. Investigated cases are located along the line separating

corrugated flamelets and distributed / thin flame reaction regimes. For the selected points the regime diagram shows that the turbulent intensity is larger than the laminar flame speed. Therefore, the turbulent motion can generate fresh and burnt gas pockets leading to a wrinkled flame front. At such conditions the turbulence influences the premixed zone and the reaction zone retains its wrinkled but to a certain extent still laminar character. In addition, for *Da* values larger than one the flame time scale (d/S_L) is smaller than the characteristic eddy time (l_I/u'). Consequently, the turbulence does not have a strong impact on the flame structure. However, the Kolmogorov scales appear to be smaller than the flame thickness, hence the flame is not laminar having a wrinkled character. These findings were confirmed also experimentally [18] showing that even though the modifications of contour spacing or curvature are not singnificant at elevated turbulence level the turbulent effects still predominate and are determinative for the burning rate increase.

BMEP [bar]	6.9	10.9	13.6	17.3
ϕ	0.36	0.40	0.41	0.46
p_{cyl} [bar]	41	56	68	75
u' [m s^{-1}]	3.83	4.31	4.656	5.041
S_L [m s^{-1}]	0.45	0.50	0.53	0.65
u'/S_L	8.42	8.64	8.71	7.80
l_I [m]	0.0144	0.0144	0.0147	0.0150
δ [m]	4.81E-05	4.39E-05	4.10E-05	3.39E-05
l_I/δ	2.99E+02	3.28E+02	3.59E+02	4.43E+02
Da	36	38	41	57
Ka	1.41	1.40	1.36	1.03
Re_T	2.52E+03	2.83E+03	3.13E+03	3.45E+03
K	0.222	0.220	0.213	0.162
η_k [m]	4.05E-05	3.71E-05	3.52E-05	3.33E-05

Table 2 Overview of turbulent flame relevant parameters for selected operation points

The turbulent regime of thin reaction zones is characterized by enhanced oxidation rate resulting from the wrinkled flame structure and need to be considered for the turbulent flame velocity correlation. Lewis number *Le* represents a non-dimensional measure for the flame curvature as consequence of the flame stretch. Effects of molecular diffusion at high turbulence intensities on turbulent premixed flame were investigated by Dinkelacker et al. [24]. In this respect, an effective *Le* needs to be assumed for considering the concentration of fuel in oxidizer. The proposed algebraic relation is derived from a transport equation with the density-weighted mean reaction progress variable and yields equation (40), which is employed to the present model.

$$\frac{S_T}{S_L} = 1 + \frac{0.46}{Le} Re_T^{0.25} \left(\frac{u'}{S_{L,0}}\right)^{0.3} \left(\frac{p}{p_0}\right)^{0.2} \tag{40}$$

As discussed above, the Lewis number *Le* characterizes the turbulent premixed flame structure and thus impacts the final burning rate substantially. In order to determine its effective value, an analytical correlation (41) following the approach in [25] is used taking into account both Lewis numbers of the unburned fuel and oxidizer and their concentrations.

$$Le_{eff} = 1 + \frac{(Le_{O2} - 1) + (Le_{CH4} - 1)\big(1 + \beta(\Phi - 1)\big)}{2 + \beta(\Phi - 1)} \tag{41}$$

where Φ is equal to ϕ for fuel-rich mixtures and $1/\phi$ for fuel-lean conditions. Such definition allows considering excess air ratio changes related to the load variation or changing operating conditions. In this way instability effects occurring especially with very lean mixtures can be considered in the phenomenological combustion model.

6. Results

6.1 Diesel Model Results

Diesel combustion is validated against experimental data from engines varying in bore size, compression ratio or number of injectors. *Table 3* summarizes key engine parameters of three different large 2-stroke diesel marine engines at CMCR operation. All are equipped with exhaust turbocharger with fixed geometry turbine and feature electronically controlled common-rail injection system as well as variable exhaust valve actuation. Whereas the RT-flex50DF has two peripheral injectors and reduced CR optimized for dual fuel operation RT-flex60 and W-6X72 have three injectors per cylinder to ensure proper atomization and distribution of the injected fuel amount and high CR for optimum engine efficiency. These engine types were selected intentionally to cover various specifications and sizes of large marine low speed engines.

Engine type	**RT-flex50DF**	**RT-flex60**	**W-6X72**
Number of cylinders	6	4	6
Bore [mm]	500	600	720
Stroke [mm]	2050	2250	2500
Compression ratio	12.0	18.45	18.8
Engine speed [rpm]	124.0	114.2	84.8
BMEP [bar]	17.3	21.0	20.5
Injectors per cylinder	2	3	3
Injector nozzle	212.DF.V03	213.LLb12h	220.A2.Std

Table 3 Diesel engines specification overview at CMCR operating conditions

The developed modeling approach is integrated in the 1D engine cycle simulation tool GT-Power by means of a user subroutine. Input parameters such as in-cylinder conditions, injection profiles or model constant are defined directly in the user code or are transferred through the user code reference object and user code harness variables. The state of the art two-zone cylinder model is adopted and the thermodynamics are calculated with the predefined real-gas model based on Redlich-Kwong equation of state. For diesel operation a user heat transfer model is employed considering both convective and radiative heat fluxes.

Fuel injection pressure represents the key parameter determining the resulting burn rate impacting spray morphology, evaporation and mixing process. Increasing the injection pressure ultimately raises the turbulence intensity, which in turn accelerates both mixing and oxidation processes. From the engine performance perspective, proper adjustment of fuel injection pressure allows to find an optimum for combustion efficiency and emissions formation. Therefore, the model response to injection pressure variation is essential with respect to model application for optimization studies. Prior to analyzing the effect of rail pressure on the combustion itself the injection rate needs to be determined. For the fast running engine models, the use of an injection rate map has proven beneficial especially due to low computational demand and high flexibility. The AMESim simulation code was used to run detailed hydraulic simulations of the common-rail

injector. The reliability of the numerical results was tested through a comparison between numerical and experimental results when using marine diesel oil (MDO) as fuel. Subsequently, broad variations of rail pressure from 500 to 1600bar and energizing time from 10 to 30ms were used for injection rate map definition.

To assess the performance of the developed combustion model, both crank angle resolved HRR and key performance figures have been evaluated. Key variables such as engine load, fuel rail pressure, nozzle execution, injection patterns or engine type were varied and model results compared with experiments. *Figure 13* shows the simulated specific HRR and cylinder pressure history for a load variation on the RT-flex60 engine compared with measured data.

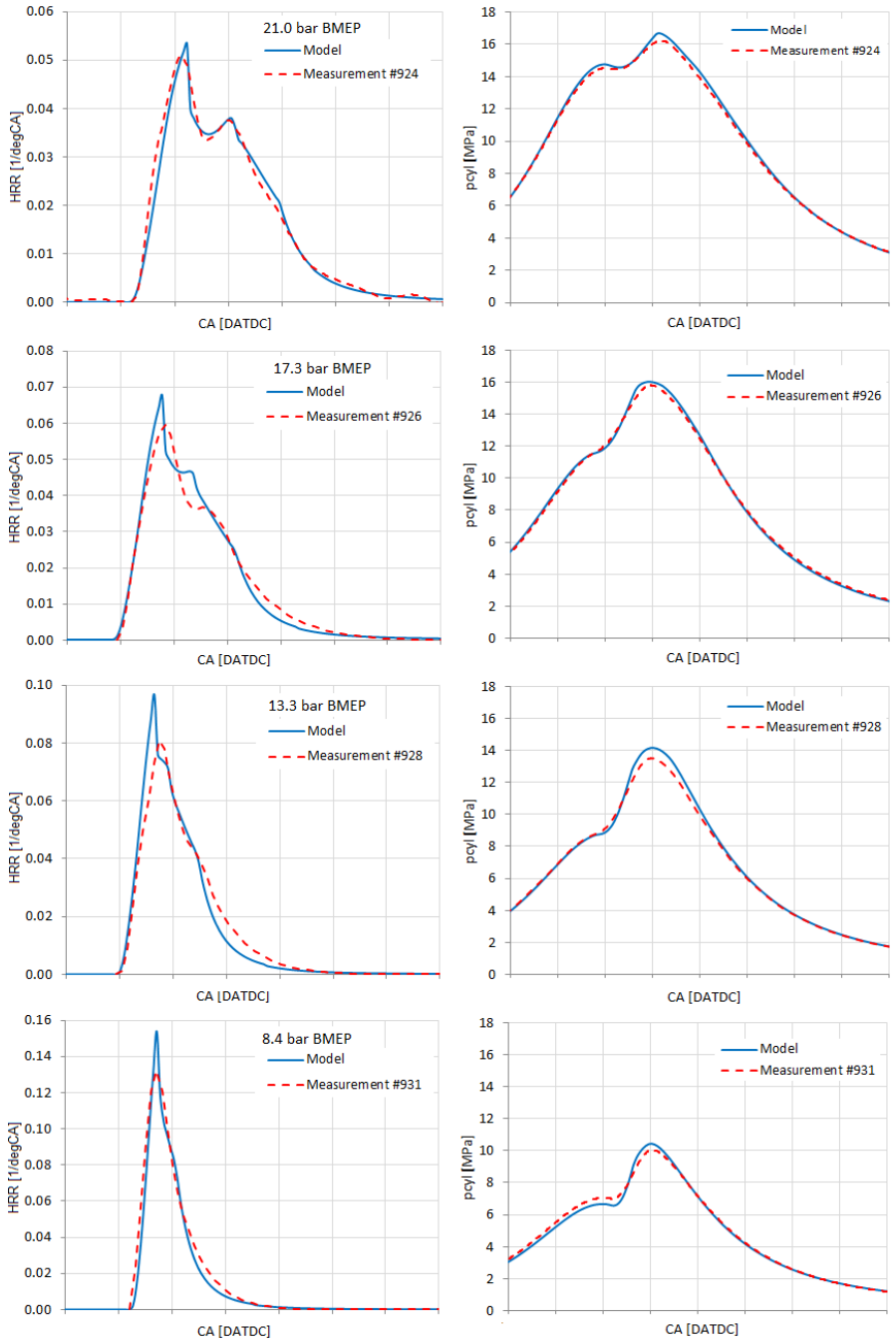

Figure 13 Predicted and measured specific HRR and cylinder pressure for RT-flex60 load variation

At every load point the combustion onset, temporal progress, point of interaction as well as the late combustion phase are well captured by the model. Especially the full load point simulation at

21.0 bar BMEP reproduces the experimental ROHR profile in a very plausible way. When reducing the load, the initial phase of the heat release tends to be somewhat overpredicted. Consequently, also the point of spray interactions occurs earlier than measured. This also causes the late burning phase to be slightly accelerated. However, in the late combustion phase after the fuel injection is terminated the turbulence level dissipates very fast and the burn rate progress becomes uncontrolled. In the present model the gradient of the burn rate tail can be adjusted by both controlling the burn rate recovery after the spray interaction and turbulence dissipation coefficient.

Figure 14 summarizes the results of the complete set of variations considered in the present validation study (34 measurements from various engine types) in the form of six plots of key performance parameters.

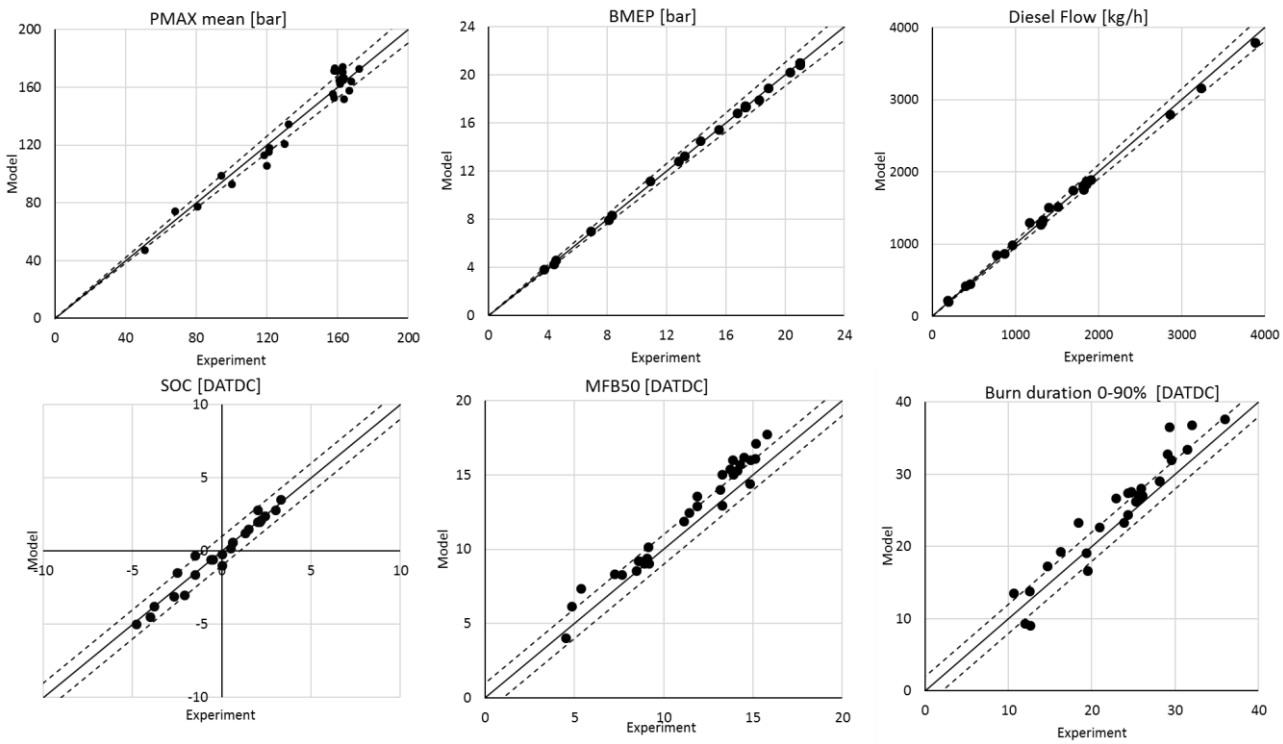

Figure 14 Performance of the diesel model with respect to key parameters

For every plot the x-axis shows experimental results and the y-axis model predictions, with dashed lines denoting error bands of 1% (upper row) and 1 respectively 2 (rightmost diagram) degrees crank angle (bottom row). The simulation is targeting the measured BMEP while the fuel flow is determined by a PID controller. Upper left and right plots illustrate maximum firing pressure PMAX and the determined diesel fuel flow both predicted mostly within the 1% error band. The remaining plots present model performance in terms of ignition delay and combustion phasing. Start of combustion (SOC) reflects the ignition delay calculation where the error does not exceed one crank angle unit. Note that data points above the full line center axis refer to the RT-flex50DF engine, on which a longer ignition delay is observed than determined by the model. The combustion phasing is characterized by the crank angle position of 50% fuel mass fraction burned (MFB50). For the majority of the cases predicted MFB50 lies within the ±1°CA accuracy interval. However, the model predictions of combustion phasing tend to be slightly overestimated. This becomes even more pronounced when considering the combustion duration determined as crank angle interval between the start of combustion and 90% of fuel mass burned. Generally, the spread gets larger and most of the calculated points are located on the edge of the ± 2°CA

accuracy band. This indicates that during the late combustion phase the calculated heat release may proceed at a lower rate than during the experiment. Nonetheless, one may conclude that the model accuracy is at a good level and in spite of engine type related differences in model HRR prediction, general model performance is meeting the requirements for fast running and generic engine cycle simulation.

6.2 Dual Fuel Model Results

The proposed model has been extensively validated against experimental data of full scale large 2-stroke low speed DF engines. Data from two different DF engines types were utilized for comparing simulation and test results. *Table 4* provides an overview of key design specifications and major performance parameters at CMCR operation for both engine types. A dual fuel 2-stroke engine is equipped with electronically controlled common rail fuel injection, electro-hydraulic exhaust valve actuation, direct gas admission valves (GAV) and pilot combustion chambers (PCC) accommodated in the cylinder head. The RT-flex50DF engine was used for the dual fuel concept development to determine optimum performance parameter settings, turbocharger matching and define the gas admission relevant component design. During the concept development phase, numerous engine specifications and concepts were investigated and assessed. A broad database of experimental data has allowed comprehensive model verification over a wide range of engine settings and operation conditions.

Engine type	**RT-flex50DF**	**W-6X72DF**
Number of cylinders	6	6
Bore [mm]	500	720
Stroke [mm]	2050	2250
Compression ratio	12.0	12.0
Engine speed [rpm]	124.0	87.2
BMEP [bar]	17.3	17.3
GAV per cylinder	2	2
Injectors / PCC per cylinder	2 / 2	3 / 2

Table 4 Dual fuel engines specification overview at CMCR operating conditions

The dual fuel combustion model developed within the present work was integrated into a 1D simulation tool by means of a user routine analogously to the approach used for the diesel combustion model. The cycle simulation results and predicted heat release rates were used for comparison with measured data from the RT—flex50DF test engine. Points for validation were selected for encompassing a wide variation of input parameters such as engine load, equivalence ratio and gas pressure, to ensure appropriate robustness of the model.

Figure 15 demonstrates the performance of the simulation model for selected steady state engine operation points on the propeller curve. The calculated specific HRR and cylinder pressure traces are compared with experimental data. Evidently, the model predictions are on a very good level over the entire load range. Especially the pilot combustion peak can be captured correspondingly to the measurement. Similarly, the HRR shape of the main premixed combustion phase calculated based on the correlations for laminar and turbulent flame velocity defined in previous sections shows good agreement with the measurements. In terms of ignition delay determination reliable results have been achieved at high and medium engine load operation. At low load the accuracy can still be considered acceptable in view of the known limitations of the applied methodology. The observed over-prediction is attributed mainly to the cylinder discretization constraints which

do not allow capturing the spatial differences of temperature and fuel concentration in sufficient detail.

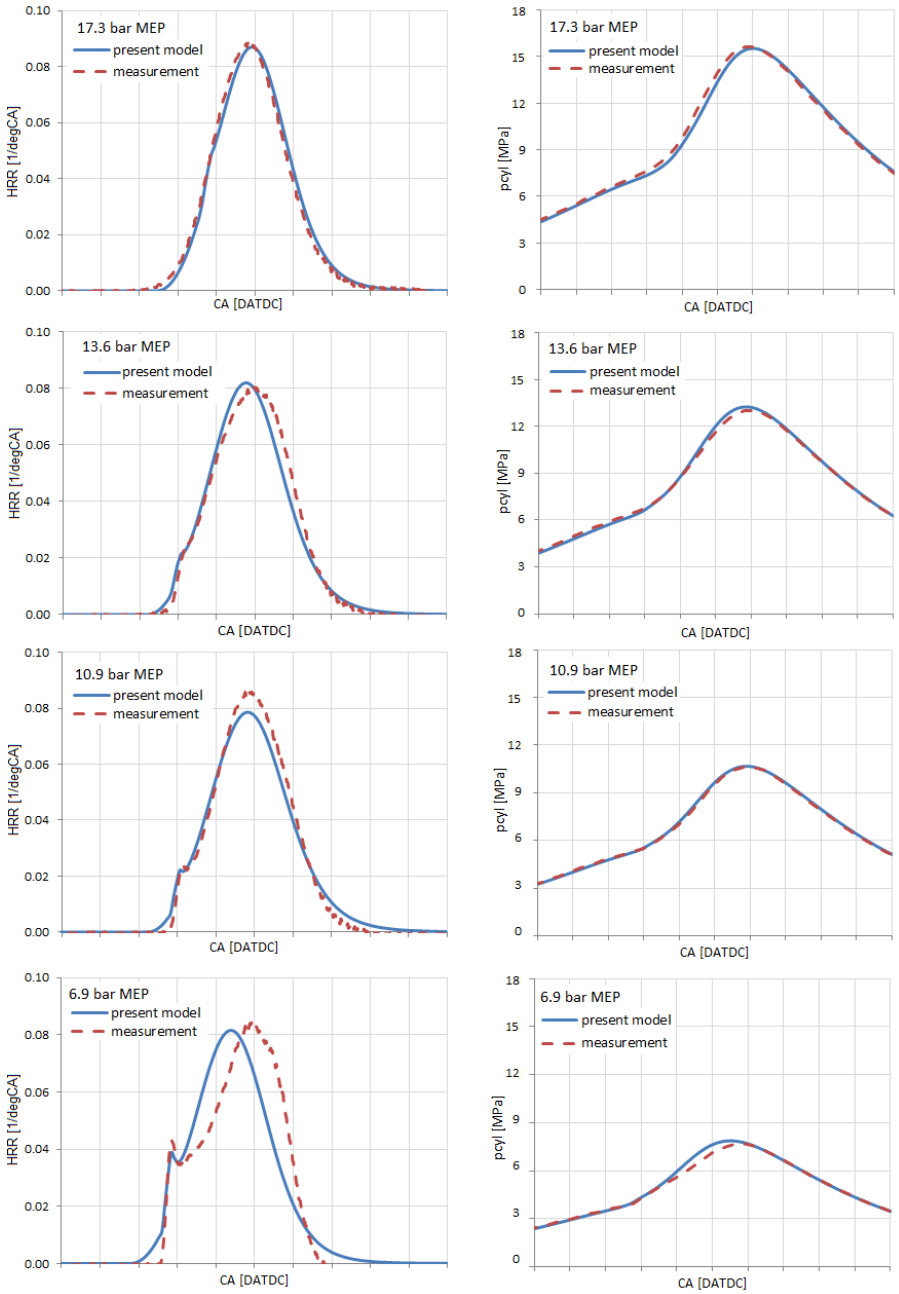

Figure 15 Predicted and measured specific HRR and cylinder pressure for RT-flex50DF engine load variation

Key engine performance parameter predictions compared to experimental data are summarized in *Figure 16* for 50 measurements used for model validation, similar to Figure 15 above. The selected points cover a broad spectrum of engine operation conditions. The averaged PMAX values predicted by the model are mostly within the 1% error band. Even higher accuracy is shown for the engine power calculation in terms of both BMEP and gas flow. The three bottom plots show how well the calculated burn rates match experimental results in terms of ignition delay and combustion phasing. Start of combustion (SOC) refers directly to the ignition delay calculation fidelity. Only for very few measurement points the error exceeds 1°CA and hence the ignition delay prediction can be considered reasonably accurate. Also for the MFB50, the majority of points lies within the ±1°CA interval whereas for some cases the model calculates earlier

combustion phasing than measured. However, also those cases are located within a ±2°CA accuracy band. The same prediction accuracy is reached for the overall combustion duration determined as the crank angle interval between 5% and 90% of fuel mass burned. The conclusion that the developed model predicts all key parameters with good accuracy to be used for generic 1D engine cycle simulations is hence well justified.

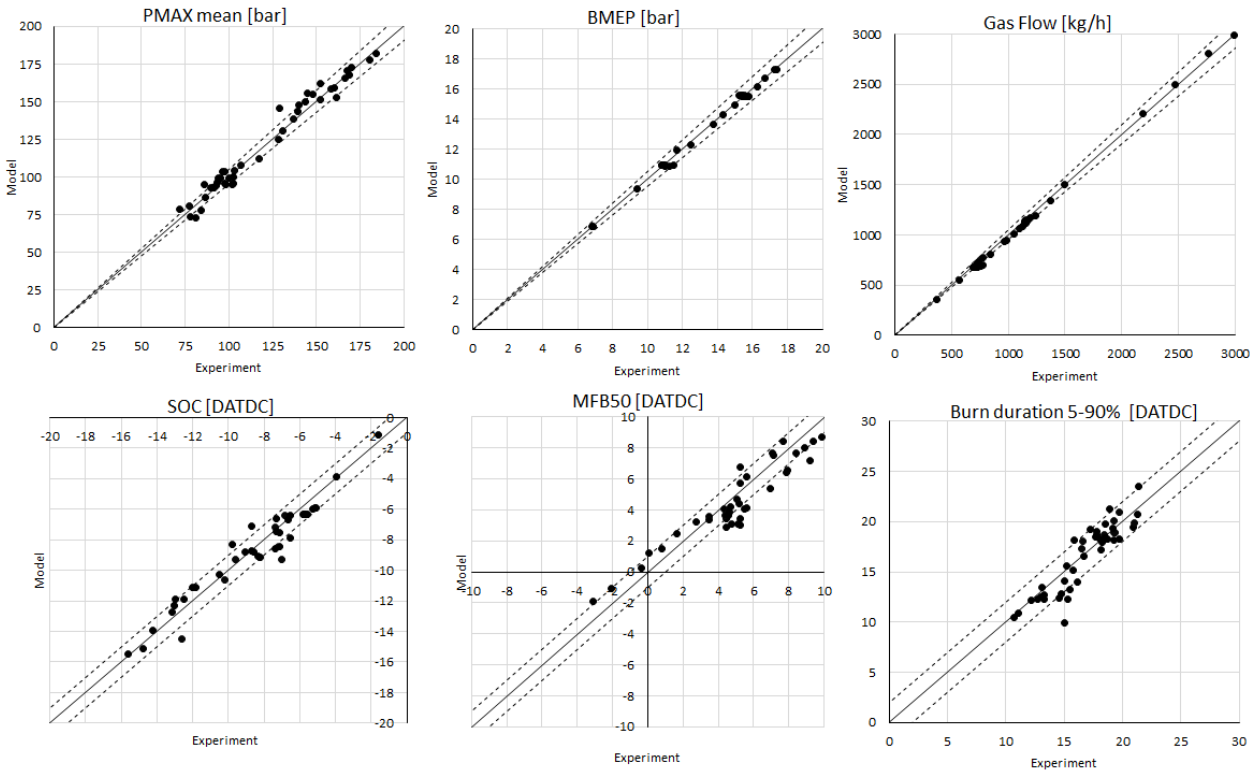

Figure 16 Performance of the DF model against measurement points with respect to key parameters

7. Conclusions

Following the thesis objectives phenomenological aspects of combustion in large low speed 2-stroke marine engines with respect to both diesel and dual fuel combustion were thoroughly assessed on the basis of results of extensive experimental investigations as well as detailed CFD simulations. The key findings from this assessment were employed for developing models describing combustion phenomenology on the basis of various submodels relevant to spray morphology, mixture formation, ignition delay, turbulence, spray interactions or premixed flame velocity. These submodels were first individually validated against experimental data or dedicated computational studies and the resulting complete models then integrated in the form of user combustion routine in a commercial 1D engine cycle simulation tool. Final model calibration was done by comparing the predicted heat release data with real engine results. Regarding key performance figures, the modeling methodology has shown good level of accuracy and predictivity.

The state of the art study has revealed that in spite of numerous models available especially for diesel combustion there is a gap in terms of fast and predictive combustion models in the segment of large 2-stoke marine engines. This gap is even larger for lean burn DF combustion in such engines with direct low pressure gas admission and pre-chamber pilot fuel ignition, which could previously not be simulated at all in a fast and predictive way due to the lack of any suitable phenomenological approach. This is due to the complexity of the combustion systems involved, which is associated with the presence of multiple peripheral injectors in the diesel case and the deviation from stoichiometric and homogeneous mixture composition in the DF case. In order to formulate a generic modeling concept, a quasi-dimensional approach was identified as prerequisite to account for spatially resolved phenomena such as interactions of diesel sprays or ignition delay of premixed charge. Therefore, the proposed simulation methodology represents a novel approach for fast running physics based models for diesel and dual fuel combustion regimes applicable in such engines.

Within the diesel combustion model both zero-dimensional turbulence and quasi-dimensional spray interaction models are essential with respect to overall model accuracy. The spray formation and interaction model was developed adopting results of elementary spray research carried out in the spray combustion chamber (SCC) and multidimensional CFD simulations. Individual submodels for spray penetration, dispersion and ignition delay were validated against experiments. For consistency purpose, these submodels were not further adjusted for optimization of the predicted HRR. The spray interaction model is based on quasi-dimensional resolution of spray penetration within the combustion space and the amount of fuel available for the diffusive combustion is related to the ratio of free and interacted spray area. Both premixed and diffusion combustion models were derived adopting the time scale approach. Corresponding model constants were tuned primarily with respect to experimental heat release rate measured on the RT-flex60 engine for load and key parameter variations.

Ignition delay predictions are in very good agreement with start of combustion observations for the engine cases simulated. Note that, for the large low speed 2-stroke engine the premixed combustion phase is mostly negligible. Hence, the transition between both combustion regimes cannot be assessed in detail. Nonetheless, single cases at reduced compression ratio confirm the validity of the resulting heat release rate patterns in view of the adequate premixed peak predictions. The spray interaction onset is well captured by the model and corresponds with the measured start of the HRR restriction due to local lack of oxidizer. Likewise, the HRR recovery

phase and the associated acceleration of the heat release rate is predicted in line with measurements, even if model application to other engine types yielded somewhat advanced onset of spray interactions and partial overprediction of the HRR recovery phase. The sensitivity study covering a broad variation of engine parameters confirmed the generic character of the developed mode. High quality of HRR and engine performance predictions was achieved for load and fuel rail pressure variations. However, nozzle execution specific differences can be captured only by trend but not in terms of exact spray interaction magnitude and late combustion phase progress. Similarly, predictions for the implemented sequential injection strategy were not sufficiently accurate. Except for such very special cases, the results of key engine performance figures and combustion phasing predictions are very good and the approach hence meets the requirements for fast and predictive engine cycle simulations.

Analogously, the DF model is strongly dependent on the appropriate description of turbulence-chemistry interaction effects as well as the proper representation of quasi-dimensional aspects associated with the deviation from homogeneity of the premixed charge and the associated impact on ignition. The model was derived by applying premixed and turbulent flame theory to the present case of a large low speed engine. Due to the limited experimental database directly meeting requirements of large 2-stroke marine engines, literature research and detailed kinetic models were utilized for model derivation. Individual submodels were validated against results of multi-dimensional CFD investigations. Ignition delay was modeled for both pilot diesel injection and the gaseous fuel. The latter relates closely to the scavenging and gas admission process that take place simultaneously. Here, a cylinder discretization was proposed to allow for spatial differences in burn gas concentrations, temperature and the equivalences ratio of the gas-air mixture. Subsequently, the locally resolved conditions are utilized for determining the auto-ignition of the gaseous fuel substituted by methane in present study.

Predictions made my means of this model are well in line with experimental observations made in the context of extensive parametric variations conducted on a test engine. By nature, deviations are somewhat larger than for the diesel model but computed ignition delay is in good agreement with start of combustion detections on the engine. The same applies for the HRR progress parameters investigated, even if, for some cases, the model tends to predict slightly faster combustion than observed in the tests. Nonetheless, the conclusion that the developed model predicts all key parameters with sufficient accuracy to be used for generic 1D engine cycle simulations is well justified.

The relevance of an appropriate representation of turbulence for both models cannot be overemphasized. Reducing the k-ε turbulence model to a zero-dimensional form for isotropic and homogeneous turbulence has proven successful as was demonstrated by the quality of the predicted mean cylinder TKE. TKE is decisive in terms of diffusion combustion prediction as well as turbulent flame velocity determination. Therefore, the relevant turbulence generation effects need to be properly accounted for, including the flow through the inlet ports, gas admission for the DF as well as fuel injection for the diesel case. In this respect the initial fuel injection rate profile together with the effective injection pressure need to be properly defined.

There are several features and general limitations of proposed methodology for combustion modeling that are worth noting. By nature, the pronounced fidelity compromise compared to multidimensional CFD models is indisputable. With respect to the reduced zero-dimensional turbulence model, the limited prediction accuracy showed negligible impact on simulated heat release rate. On the other hand, the lack of spatial resolution has a direct impact on both ignition delay and flame speed computation. Concerning the generic validity, in contrast to the author’s

intention to do without artificial model constants, the application to different engines types and bore sizes requires yet some model adaptations. This is prerequisite for both diesel and dual models due to differences in ignition behavior, turbulence generation and dissipation or spray interactions related to injector number or in-cylinder flow. Especially the application of the spray interaction model on various engines types has unveiled several deficiencies linked to the quasi-dimensional model. With respect to the DF combustion model, the model at present cannot predict knock and neglects the impact of gas quality (MN) on flame propagation. Furthermore, the validity of emission predictions in terms of nitric oxide and soot formation could not be confirmed due to the limited scope of the present work. Nevertheless, corresponding models were outlined and can be easily implemented within the user code structure and subsequently integrated in the 1D simulation tool.

The integration of the models into the GT-Suite simulation environment has proven the feasibility of the proposed methodology to be effectively used for fast engine cycle studies of multiple cases or extensive DoE runs. Thanks to the generic character of the combustion model this can be done already in the early phases of a development process. The simulation methodology developed in the present thesis has been successfully demonstrated on a variety of 1D fast running models and has been published and well accepted at SAE World Congress 2016 [26] and Gamma Technologies user's conference [27]. Moreover, case studies using the proposed methodology for combustion simulation have demonstrated the potential of the developed modeling approach for industry applications and we envisage the application of the proposed simulation methodology for optimizing actual large 2-stroke engines and integrated marine propulsion systems.

References

1. International Maritime Organization, “Annex VI of MARPOL 73/78: Regulations for the Prevention of Air Pollution from Ships and NOx Technical Code”, IMO-664E, London, 1998.
2. Ott, M., Nylund, I., Alder, R., Yamada, T., Hirose, T., Umemoto. Y., “The 2-stroke low pressure Dual-Fuel technology: from concept to reality”, CIMAC Congress 2016, Helsinki, Paper No. 233, 2016.
3. Von Rotz, B. et al., „Comparative Investigations of Spray Formation, Ignition and Combustion for LFO and HFO at Conditions relevant for Large 2-Stroke Marine Diesel Engine Combustion Systems”, CIMAC Paper No. 253, CIMAC Congress Helsinki, 2016.
4. Von Rotz, B., Herrmann, K., and Boulouchos, K., "Experimental Investigation on the Characteristics of Sprays Representative for Large 2-Stroke Marine Diesel Engine Combustion Systems," SAE Technical Paper 2015-01-1825, 2015.
5. Chmela, F., Orthaber, G. C., “Rate of Heat Release Prediction for Direct Injection Diesel Engines Based on Purely Mixing Controlled Combustion”, SAE Paper 1999-01-0186, 1999.
6. Hiroyasu, H., “Diesel Engine Combustion and Its Modeling”, International Symposium COMODIA 94, Japan, 1994.
7. Hiroyasu, H., Arai, M., “Structures of Fuel Sprays in Diesel Engines”, SAE Technical Paper 900475, 1990.
8. Kuleshov, A. S., “Multi-Zone DI Diesel Spray Combustion Model for Thermodynamic Simulation of Engine with PCCI and High EGR Level”, SAE Paper 2009-01-1956, 2009.
9. Liu, Z., Karim, G.A., “Predictive Model for the Combustion Process in Dual Fuel Engines”, SAE Technical Paper 952435, 1995.
10. Naber, J. D., Siebers, D., “Effects of Gas Density and Vaporization on Penetration and Dispersion of Diesel Sprays”, SAE Paper 960034, 1996.
11. Spalding, D.B., “The Combustion of Liquid Fuels”, Fourth Symposium (International) on Combustion, The Combustion Institute, 1953.
12. Varde, K.S., Popa, D.M., “Diesel Fuel Spray Penetration at High Injection Pressures”, SAE 830448,1983.
13. Faeth, G.M., “Current Status on Droplet and Liquid Combustion”, Progress in Energy and Combustion Science 3, p. 191-224, 1977.
14. Weisser, G. et al., “Integrating CRFD-Simulations into the Development Process of Large Diesel Engines: A Status Report”, CIMAC Paper No. 05.09, 1998.
15. Weisser, G., “Modelling of Combustion and Nitric Oxide Formation for Medium-Speed DI Diesel Engine: A Com-parative Evaluation of Zero- and Three-Dimensional Approaches”, Diss. ETH No. 14465, 2001.
16. Bargende, M. et al. „Turbulenzmodellierung für quasi-dimensionale Arbeitsprozessrechnung“, FVV Informationstagung Motoren, 2014.
17. Stringer, F. W., Clarke, A. E., Clarke, J. S., “The Spontaneous Ignition of Hydrocarbon Fuels in a Flowing System,” Symposium Diesel Combustion, Proc. Inst. Mech. Eng., 184 pt. 3J., 1969.
18. Nakagawa, H., Oda, Y., Kato, S., Nakashima, M., Tateishi M., „Fuel Spray Motion in Side Injection System for Diesel Engines“, COMODIA 90, p.281-286, 1990.
19. Macek, J., Steiner, T., “Advanced Multizone Multi-dimensional Models of Engine Thermaerodynamics”, Proceedings of 21st CIMAC International Congress on Combustion Engines, 1995.
20. Witt, M., Griebel, R., „Numerische Untersuchung von laminaren Methan-Luft-Vormischflammen“, Internal report, Paul Scherrer Institut, 2000.
21. Tap, F., Schapotschnikow, P., Ramaekers, G., ”Auto-ignition and premixed flame databases”, Technical report, Dacolt, 2012.

22. Bradley, D., Lau, K-C., Lawes, M., “Flame stretch rate as a determinant of turbulent burning velocity”, Philosophical Transaction of the Royal Society of London A, vol. 338, p. 359-387, 1992.

23. Peters, N., “Turbulent Combustion”, Cambridge Univ. Press, Cambridge, UK, 2000.

24. Dinkelacker, F., Manickam, B., Muppala, S.P.R., “Modelling and simulation of lean premixed turbulent methane/hydrogen/air flame with an effective Lewis number approach”, Combustion and Flame, vol. 158, p1742-1749, 2011.

25. Emani, B., Liu, R., Ting, D.S.K., Checkel, D., “A Numerical Study on the Burning Velocity of a Spherical, Premixed Methane-Air Flame”, SAE Technical Paper 2005-01-1124, 2005.

Author’s Publications and Work

26. Cernik, F., Macek, J., Dahnz, C., and Hensel, S., "Dual Fuel Combustion Model for a Large Low-Speed 2-Stroke Engine," SAE Technical Paper 2016-01-0770, 2016.

27. Cernik, F., “Integrated 1D Simulation for a Large Low-Speed 2-Stroke Marine Engine”, Proceedings GT-Suite Users Conference, 2015.

28. Cernik, F., Macek, J., Weisser, G., Schmid, A., Von Rotz, B. "Phenomenological Diesel Combustion Model for Large 2-stroke Marine Engines", submission in progress.

29. Cernik, F., Fritz, J., JS, R., "High Turndown Injection for High Speed Dual Fuel Reciprocating Engines", GE Global Research, Internal Manuscript eMR # : 2016-12-29-32172, 2016.

30. Author’s research work related to the dual fuel combustion concept development for large 2-stroke engines has contributed to the “Marine Engine of The Year” award for X-DF engines at the Marine Propulsion Awards 2017.

Abstract

A phenomenological simulation methodology for combustion modeling of both liquid and gaseous fuels for large low speed 2-stroke marine engines is developed and validated within the present study. The work incorporates modeling concepts for diesel and dual fuel combustion aiming for a physics based and generic model structure. Phenomenological aspects of these concepts are theoretically investigated and considered individually in respect of specifics of large uniflow scavenged 2-stroke engines. Individual aspects of fuel introduction, mixing, ignition and oxidation are taken into consideration with respect to multiple peripheral injectors, uniflow scavenging with imposed swirl or direct low-pressure gas admission. Implementation of the resulting models into a commercial 1D simulation tool in form of a user routine allows fast cycle simulation of full scale engine models or integrated marine power systems at a good level of fidelity. Hence, the proposed method enables the computationally effective optimization of complex propulsion systems under both steady and transient operating conditions.

The quasi-dimensional model proposed for diesel combustion is capable of accurate predictions in terms of heat release rate and engine performance figures based on an imposed injection profile. The model takes into account the specific design features of the combustion space in large two-stroke engines such as multiple decentralized fuel injectors or intake air swirl. One of the most important characteristics considered by the model is the methodology for capturing interactions among individual sprays and an appropriate adjustment of the locally effective air excess ratio, as the available oxygen is predominant for combustion progress. If the spray is enclosed by the burned gases of sprays from a neighboring injector, the burn rate is restricted and later recovered in case suitable conditions are restored. In order to reproduce this behavior, spatial resolution of the combustion chamber is considered and transformed into a quasi-dimensional and solely mathematical description. The final burn rate is then determined by a time scale model employing a simplified zero-dimensional turbulence model considering a typical integral length scale. The availability of fuel ready to be oxidized is constrained by evaporation, mixing and spray interactions. Extensive validation is performed against data from experimental investigations in a spray combustion chamber (SCC) and full-scale engine data. The computation is executed by means of an integrated combustion subroutine using a dynamic link library interface with the 1D engine model. Instantaneous import of in-cylinder conditions and injection rates enables immediate prediction of heat release rate. The validity of the model predictions under various operating conditions is confirmed for several Wärtsilä low-speed marine engine types.

The dual fuel phenomenological combustion model accounts for both diffusion combustion of the liquid pilot fuel and the flame front propagation through the gaseous premixed charge. In the context of the pilot fuel model a common integral formulation defines the ignition delay whereas a time scale approach is incorporated for the combustion progress calculation. In order to capture spatial differences given by the scavenging process and the admission of the gaseous fuel, the cylinder volume is discretized into a number of zones. The laws of conservation are applied to calculate the thermodynamic conditions and the fuel concentration distribution. Subsequently, the ignition delay of the gaseous fuel-air mixture is determined by the use of tabulated kinetics and the ensuing oxidation is described by a flame velocity correlation. Computational concepts for both laminar and turbulent flame velocities are determined based on conditions characteristic for large 2-stroke marine engine operation. Comprehensive theoretical studies and computational assessments have been accomplished to derive appropriate correlations for propagation of both laminar and turbulent flames. The resulting heat release rates and pressure traces are validated against experimental engine data. Sensitivity studies of major parameters related to combustion

such as scavenging temperature, equivalence ratio, pilot timing or compression ratio are performed. Performance predictions are tested for several engine types and show good level of agreement with measurements.

The proposed methodology generalizes phenomenological aspects of combustion in large low speed 2-stroke marine engines with focus on diesel and dual fuel combustion under both steady and transient operation conditions. The modeling approach has proved to be viable for the optimization of present and future marine propulsion systems. Apart from the application to a standalone engine model also an entire propulsion system with integration of hydraulic models for fuel injection or exhaust valve actuation has been modeled. The user routine based model structure allows performing standalone or system integrated calculations and thus facilitates direct utilization for engine optimization. Furthermore, options for model extension in terms of emission modeling are outlined. The fundamental scientific contribution of the present work relies on the generation of a better understanding of the complexity of combustion processes in large low speed 2-stroke marine engines, the identification of the governing phenomena and the derivation of suitable modelling approaches for reducing the complexity to a level allowing the fast but yet generic simulation of large 2-stroke engine combustion.

Anotace

Disertační práce popisuje vývoj a validaci fenomenologické metodiky simulace spalování kapalných a plynných paliv ve velkých pomalobežných dvoutaktních lodních motorech. Práce zahrunuje kocept simulace dieselového a duálního neboli dvoupalivového hoření z cílem vypracování fyzikálně zobecněného modelu. Fenomenologické aspekty těchto konceptů jsou teoreticky vyhodnoceny z hlediska specifik pomaloběžných dvoutaktních motorů se souproudým vyplachováním. Začlenění modelu do 1D simulačního softwaru GT-Suite formou uživateského programu umožňuje časově nenáročné výpočty oběhu pro samostatný model motoru nebo celkových integrovaných lodních pohonych systémů s požadovanou přesností. Tímto je umožněna efektivní optimalizace lodních pohonů při stacionárním a transientních podmínkách.

Kvazidimenzionální model navržen pro dieselové spalování umožňuje predikaci průběhu hoření a výkonových parametrů motoru na základě průběhu vstřiku paliva. Model zohledňuje koncepci spalovacího prostoru velkého dvoutaktního motoru s několika decentralizovanými vstřikovači a vířivým vyplachovním. Zásadní součástí dieselového modelu jsou interacke jednotlivých paprsků vstřiku ovlivňující lokální přebytek vzduchu, který je určující pro průběh spalování. V případě vzájemného překrytí paprsku vstřiku a spalin je průběh hoření zpomalen. K zotavení hoření nastává když je obnoven dostatečný přebytek vzduchu na základě rodílu rychlostí paprsku vstřiku a spalin. Pro dosažní těchto požadavků modelu je spalovací prostor popsán kvazidimenzionálně, což umožňuje řešení průniku a interakce jednotlivých parpsků vstřiku. Celkový průběh hoření je určen pomocí časového měřítka hoření s využitím bezrozměrného modelu turbulence a jejího integrálního měřítka. Palivo dostupné pro hoření je definované průběhem vypařování, míšení a interakcemi parpsků vstřiku. Model dieselového spalování je kalibrován s využitím experimentálních dat naměřených ve spalovací komoře (SCC) a na motoru. Samotný výpočet probíhá formou integrace uživatelského programu do 1D modelu motoru, která umožňuje okamžitou výměnu potřebných paremetrů pro rychlou predicaci průběhu hoření. Validita výsledků metodiky dieselového spalování je ověřena pro několik typů pomaloběžných dvoutaktních motorů Wärtsilä.

Fenomenologický model duálního spalování v sobě zahrnuje jak model difuzního hoření pilotního vstřiku tak model pro homogenní hoření zemního plynu. Průtah vznětu pilotního paliva je určen integrální metodou, zatímco průběh hoření je definován jeho časovým měřítkem. Za účelem modelování prostorových rozdílů způsobených procesem vyplachovní a přívodem plynného paliva je objem válce diskretizován do několika zón. Základní zákony zachování jsou využity pro výpočet přestupů hmoty mezi jednotlivými zónami a určení zónových koncentrací. Průtah vznětu plynného paliva je následně určen pomocí tabelované kinetiky. Následné hoření homogenní směsi plynu se vzduchem je popsáno rovnicí rychlosti plamene pro podmínky charakteristické pro velké dvoupalivové dvoutaktní lodní motory. Rychlost šíření plamene je popsána pro laminární a turbulentní podmínky. Analogicky vzhledem k dieselovému modelu je odvozen bezrozměrný model turbulence. Výsledné průběhy hoření jsou porovnány s experimentálními daty. Studie citlivosti výsledků modelu zahrunuje variace základních parametrů jako jsou například přebytek vzduchu, počátek pilotního vstřiku nebo kompresní poměr. Obecnost a prediktivita model duálního spalování je ověřena pro různé dvoutaktní lodní motory vzhledem k výsledkům měření.

Navržená metodika zobecňuje fenomenologické aspekty spalování ve velkých pomaloběžných dvoutaktních lodních motorů se zaměřením na dieselové a duální spalování při stacionárních a transientních provozních podmínkách. Využití navrženého simulačního přístupu pro optimalizaci bylo oveřeno pro modelování samostatného motoru i celkových pohonných systémů s integrací

hydraulických modelů vstřikovače a výfukového ventilu. Definice uživatelského programu usnadnňuje přímé využití v 1D simulačním prostředí včetně možnosti výpočtu emisí. Vědecký přínos této práce spočívá v komplexním zmapování a zobecnění spalování v pomaloběných dvoutaktních lodních motorech. Charakteristické aspekty těchto motorů týkající se vstřiku paliva, přípravy směsi a hoření jsou zohledněny z hlediska decetralizovaných vstřikovačů paliva, souproudého vyplachování válce se swirlem nebo přímého nízkotlakého přívodu plynu do válce.